JOURNAL OF PETROLOGY | VOLUME 42 | NUMBER 10 | PAGES 1813–1843 | 2001

Almandine Garnet in Calc-alkaline Volcanic Rocks of the Northern Pannonian Basin (Eastern–Central Europe): Geochemistry, Petrogenesis and Geodynamic Implications

SZ. HARANGI[1]*, H. DOWNES[2], L. KÓSA[1], CS. SZABÓ[1], M. F. THIRLWALL[3], P. R. D. MASON[4] AND D. MATTEY[3]

[1]DEPARTMENT OF PETROLOGY AND GEOCHEMISTRY, EÖTVÖS UNIVERSITY, H-1088 BUDAPEST, MÚZEUM KRT. 4/A, HUNGARY

[2]SCHOOL OF EARTH SCIENCES, BIRKBECK COLLEGE, MALET STREET, LONDON WC1E 7HX, UK

[3]DEPARTMENT OF GEOLOGY, ROYAL HOLLOWAY UNIVERSITY OF LONDON, EGHAM TW20 0EX, UK

[4]PETROLOGY GROUP, FACULTY OF EARTH SCIENCES, UNIVERSITY OF UTRECHT, BUDAPESTLAAN 4, 3584 CD UTRECHT, THE NETHERLANDS

RECEIVED AUGUST 18, 2000; REVISED TYPESCRIPT ACCEPTED MARCH 9, 2001

Almandine garnet-bearing andesites and dacites occur frequently in the Neogene calc-alkaline volcanic series of the northern Pannonian Basin (Hungary and Slovakia). They were erupted during the early stage of volcanism and occur along major tectonic lineaments. On the basis of petrographic and geochemical characteristics, garnets from these rock types are classified into (1) primary phases, (2) composite minerals containing xenocrystic cores and magmatic overgrowths and (3) garnets derived from metamorphic crustal xenoliths. Coexisting phenocrysts of primary garnets include Ca-rich plagioclase, hornblende (magnesiohastingsite to tschermakite) and/or biotite. The primary garnets have high CaO (>4 wt %) and low MnO contents (<3 wt %). They have strongly light rare earth element depleted patterns and are enriched in heavy rare earth elements. Negative Eu anomalies occur only in garnets in the more silicic host rocks. $\delta^{18}O$ values for primary garnets are 6·1–7·3‰, whereas composite garnets have elevated $\delta^{18}O$ values (>8‰). Chemical compositions of the primary garnets and coexisting minerals suggest that they crystallized at high pressures (7–12 kbar) and temperatures (800–940°C) from mantle-derived magmas. Sr–Nd isotopic compositions of their host rocks and O isotopic values of the garnets are consistent with two-component mixing between mantle-derived magma and lower-crustal metasedimentary material. The garnet-bearing silicic magmas were erupted during extension of the Pannonian Basin and the tensional stress field may have enhanced their fast ascent from lower-crustal depths, allowing preservation of early-formed almandine phenocrysts.

KEY WORDS: *almandine; garnet; calc-alkaline volcanism; geochemistry; Pannonian Basin*

INTRODUCTION

Almandine garnet is a relatively rare mineral phase in calc-alkaline volcanic rocks worldwide (Table 1). Its rarity may be due to the restricted conditions under which such garnets can form (hydrous mantle source, high-pressure crystallization from hydrous Al-rich magma) and to the particular geodynamic setting (tensional stress field), which enhances the rapid ascent of garnet-bearing melts. Green & Ringwood (1968) demonstrated that almandine-rich garnet could be a liquidus or near-liquidus mineral in silicic magmas at high pressure (9–18 kbar). Further experimental studies (e.g. Hensen &

*Corresponding author. Tel: +36-1-266-9833, ext. 2338. Fax: +36-1-266-4992. E-mail: harangi@iris.geobio.elte.hu

Green, 1973; Green, 1976, 1977, 1982, 1992; Clemens & Wall, 1981; Conrad *et al.*, 1988) showed that Ca-rich (CaO >4 wt %) and Mn-poor (MnO <4 wt %) almandine could crystallize from hydrous andesitic magmas at relatively high pressure (>7 kbar) and at temperatures of 900–950°C. Green (1977) suggested that the grossular and spessartine contents of almandine are sensitive to pressure–temperature conditions. The grossular content of garnet increases with increasing pressure, whereas a higher Mn content stabilizes garnet at shallower depths, so that Mn-rich (MnO >4 wt %) almandines can crystallize from silicic liquids at $\leq$5 kbar. Magma composition exerts a strong influence on garnet chemistry. Garnets hosted by peraluminous (S-type) volcanic rocks are CaO poor (CaO <4 wt %), whereas garnets crystallized from metaluminous (I- or M-type) magmas have higher CaO content (CaO >4 wt %). In summary, the chemistry of almandine-rich garnet is sensitive to the conditions of formation, indicating the petrogenetic importance of this mineral in volcanic rocks.

Ca-bearing almandine garnet is unstable at low pressure (e.g. Green, 1982, 1992). At shallow depths resorption of garnet begins and garnet may disappear during a long residence time in a shallow magma chamber. Therefore, the presence of primary Ca-bearing almandine in volcanic rocks suggests relatively rapid ascent of the host magma (e.g. Fitton, 1972; Gilbert & Rogers, 1989), which could be enhanced by a tensional stress field (regional extension).

Almandine occurs in Neogene calc-alkaline volcanic rocks of the Carpathian–Pannonian region of Eastern–Central Europe (Fig. 1a) and is relatively common in the Northern Pannonian Basin (Hungary and Slovakia; e.g. Brousse *et al.*, 1972; Embey-Isztin *et al.*, 1985; Lantai, 1991; Szabó *et al.*, 1999). The geodynamic setting and the relationship between volcanism and tectonic events in this region have long been the subject of debate (e.g. Lexa & Konečný, 1974; Balla, 1981; Szabó *et al.*, 1992; Lexa, 1999; Harangi & Downes, 2000). The rarity of garnet-bearing volcanic rocks in general and the experimental results pointing to their high-pressure origin suggest that their formation and eruption require particular geodynamic conditions. Therefore, garnet-bearing volcanic rocks could carry useful information concerning the geodynamics of magma genesis in this area. In addition, a detailed study of the garnets and their host volcanic rocks in the Carpathian–Pannonian region will contribute to our knowledge of the genesis of garnet-bearing magmas worldwide.

In this paper we present a petrologic and geochemical study of garnets and their host rocks from the Northern Pannonian Basin (NPB). We provide major and trace element data for the garnets and the first oxygen isotope data for igneous almandines. Interpretation of the major and trace element composition and Sr and Nd isotopic ratios of the host rocks, combined with the oxygen isotope composition of the garnets, suggests a petrogenesis involving mantle-derived host magmas and lower-crustal contamination processes. We conclude that the eruption of garnet-bearing magmas within the Pannonian Basin was related to an extensional tectonic phase.

GEOLOGICAL BACKGROUND

Calc-alkaline volcanism along the Carpathian volcanic arc took place from the Miocene to the Quaternary. Although a direct relationship has been suggested between volcanism and subduction in the East Carpathian arc (e.g. Bleahu *et al.*, 1973; Boccaletti *et al.*, 1973; Mason *et al.*, 1998), genesis of the calc-alkaline volcanic rocks of the West Carpathians is more controversial. A subduction-related genesis was proposed by Balla (1981), Szabó *et al.* (1992) and Downes *et al.* (1995), whereas Lexa & Konečný (1974), Lexa *et al.* (1993), Harangi *et al.* (1999) and Lexa (1999) suggested that melt generation was due to extension of the Pannonian Basin.

The calc-alkaline volcanic rocks of the Carpathian arc are dominantly andesites and dacites with subordinate rhyolites and basaltic andesites (e.g. Szabó *et al.*, 1992; Kaličiak & Žec, 1995; Konečný *et al.*, 1995; Mason *et al.*, 1996). Garnet-bearing volcanic rocks occur throughout the arc, but are most abundant in the west (Fig. 1a). This segment overlaps the northern part of the Pannonian Basin and comprises the Central Slovakian Volcanic Field (CSVF), the volcanic complexes of the Börzsöny and Visegrád Mts and the Cserhát and Mátra volcanic areas (Fig. 1b). Volcanism in the NPB started with eruption of medium-K to high-K garnet-bearing magmas (16·5–16 Ma; Konečný *et al.*, 1995; Harangi, 1999), followed by the eruption of garnet-free, dominantly andesitic volcanic products (Konečný *et al.*, 1995; Harangi & Downes, 2000). The garnet-bearing volcanic rocks are situated along major tectonic lines, such as the Pilis line in the southwestern Visegrád Mts, the Diósjenő line across the Börzsöny Mts, the Etes tectonic zone in the Karancs and the Central Slovakian Fault across the CSVF (Fig. 1b). Calc-alkaline volcanism terminated at $\sim$9 Ma (Pécskay *et al.*, 1995) and was followed by alkaline basaltic magmatism within the CSVF and in the Nógrád–Gömör Volcanic Field (Fig. 1b). The crust and lithosphere beneath the NPB thin gradually towards the south. The relatively thin crust (28–32 km) and lithosphere (70–90 km; Horváth, 1993) may imply that evolution of this area was influenced by the Mid-Miocene syn-rift extension of the Pannonian Basin.

ANALYTICAL TECHNIQUES

Electron microprobe data were obtained using a JEOL-733 Superprobe equipped with an Oxford Instrument

Table 1: Summary of occurrences of garnet-bearing volcanic rocks worldwide and proposed origins of the garnets; CaO content of the garnet is indicative of magma type (see Fig. 11)

Locality	Rock type	Garnet		References
		Origin	CaO content (wt %)	
Pyrenees	dacite and rhyolite (S-type)	primary phenocryst	2·8–3·05 and 6·27	Gilbert & Rogers (1989)
SE Spain	dacite (S-type* or M-type†)	restite/xenocryst* or primary†	0·40–2·90	*Zeck (1970, 1992); Munksgaard (1984, 1985); †López-Ruiz *et al.* (1977), Benito *et al.* (1999)
English Lake District	andesite, dacite and rhyolite	primary	1·26–2·16	Oliver (1956); Fitton (1972); Thirlwall & Fitton (1983)
French Massif Central	rhyodacite, rhyolite	xenocrysts (metamorphic)	0·90–1·88	Bertaux (1982)
Lipari (Italy)	andesite, dacite	xenocryst	1·56–1·79	Maccarone (1963); Barker (1987)
Central Caucasus	andesite, dacite (M-type)	primary	7·18–13·14	Tsvetkov & Borisovskiy (1980)
Greater Caucasus	andesite, dacite	xenocryst (restite)	n.d.	Popov *et al.* (1982)
Yamanogawa (Yam) and Kamitazawa (Kam), Japan	dacite (Yam; I/M-type), rhyolite (Kam; S-type)	primary	5·59–7·42 (Yam); 2·26–3·19 (Kam)	Kano & Yashima (1976)
Asio, Japan	fayalite dacite	?	n.d.	Kuno (1969)
Setouchi, Japan	andesite, dacite (I/M-type)	?	n.d.	Ujike & Onuki (1976)
Canterbury, New Zealand	dacite (M-type, Mt Somers) and rhyolite (S-type, Mt Misery)	primary and xenocryst	4·98–5·80 (Somers); 2·10–3·80 (Misery)	Wood (1974); Barley (1987)
Northland, New Zealand	andesite, dacite (M-type)	primary	5·85–9·16	Day *et al.* (1992); Green (1992)
Victoria, Australia	rhyodacite, rhyolite, granodiorite (S-type)	primary and xenocryst (restite)	0·69–1·90	Green & Ringwood (1968, 1972); Birch & Gleadow (1974); Clemens & Wall (1984)
Lesser Antilles	andesite (Morne La Plaine) to dacite (Gros Islet)	primary	4·04–5·52	Westercamp (1976); Maury *et al.* (1985); Davidson & Harmon (1989)
Trinity Peninsula, Antarctic	andesite, rhyolite (S-type)	primary	2·74–5·80	Hamer & Moyes (1982)

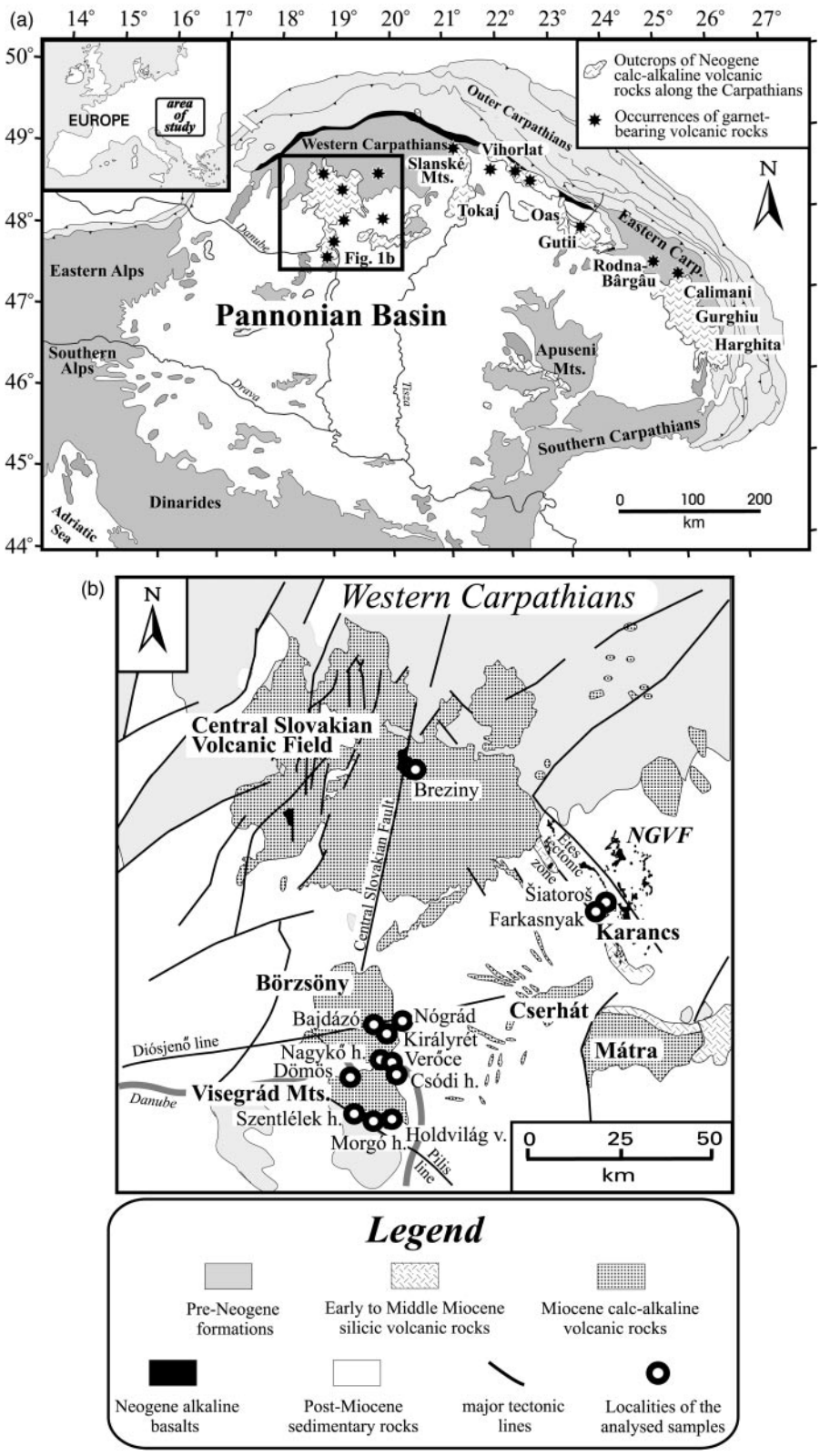

Fig. 1. (a) Occurrences of garnet-bearing calc-alkaline volcanic rocks in the Carpathian–Pannonian region; (b) localities of studied garnet-bearing calc-alkaline volcanic rock samples in the Northern Pannonian Basin. NGVF, Nógrád–Gömör Volcanic Field.

ISIS energy dispersive system (Birkbeck College, University of London) using 15 kV accelerating voltage for 100 s. Some garnet analyses were also carried out using a JEOL Superprobe JXA-8600 wavelength dispersive system at the University of Florence; compositions obtained by both methods were the same within analytical error.

Selected garnets were analysed for their O isotope composition at Royal Holloway University of London (RHUL) using a laser fluorination system attached to a VG Isotech PRISM gas-source mass spectrometer (Mattey & Macpherson, 1993). Samples (1·4–1·7 mg; 7–10 grains) of inclusion-free garnet were analysed, usually in duplicate. The samples were heated with a Nd–YAG laser in the presence of ClF_3. Yields were >92% (mostly >95%) for all the samples. San Carlos (SC) olivine was used as a secondary standard. Data, recorded as $\delta^{18}O$ values, are given with reference to Standard Mean Ocean Water (SMOW). Details of accuracy and precision have been given by Mattey & Macpherson (1993).

In situ trace element compositions of the same garnets were obtained by laser ablation inductively coupled plasma mass spectrometry (ICP-MS) at the University of Utrecht using a 193 nm ArF excimer laser ablation system (Geolas, Microlas; Günther *et al.*, 1997) in combination with a quadrupole ICP-MS instrument (Platform ICP, Micromass). The method has been described in more detail by Mason *et al.* (1999). Ablation was performed at a fixed point on the sample with a fluence of 20 J/cm^2, a laser shot repetition rate of 10 Hz and an ablation crater diameter of 120 μm, resulting in an ablated volume of 1–2 μg. Calibration was performed against NIST SRM 612 glass using the concentration data reported by Pearce *et al.* (1997). Calcium, previously determined by electron microprobe analysis at the surface of the volume removed by laser ablation, was used as an internal standard. The first 5–10 μm of material removed from the sample was not used in concentration calculations to remove the effect of surface contamination. Rare earth element results for 'in-house' garnet standards were in good agreement (better than 10% for the most homogeneous samples) with secondary ionization mass spectrometry data. Data for spots in which an inclusion had clearly been analysed were discarded.

Major and trace element compositions of the whole rocks were determined on a Philips PW1480 X-ray fluorescence spectrometer at RHUL using fused glass discs and pressed powder pellets. Details of precision have been given by Baker *et al.* (1997). Rare earth elements (REE) were analysed by ICP-MS at RHUL using the method described by Walsh *et al.* (1981). REE were separated using ion exchange columns, after fusion and dissolution of samples.

Sr and Nd isotopic compositions of the whole rocks were determined on a VG354 multicollector thermal ionization mass spectrometer at RHUL. Sample powders for Sr isotope analysis were leached in hot 6 M HCl for 1 h to remove any effects of postmagmatic groundmass alteration. Sr and Nd isotope ratios were determined in multidynamic mode as described by Thirlwall (1991). $^{87}Sr/^{86}Sr$ was normalized to $^{86}Sr/^{88}Sr = 0{\cdot}1194$ and $^{143}Nd/^{144}Nd$ to $^{146}Nd/^{144}Nd = 0{\cdot}7219$. An in-house laboratory Nd standard (Aldrich) yielded $^{143}Nd/^{144}Nd = 0{\cdot}511412 \pm 5$ (2 SD on eight analyses; equivalent to 0·511847 for the international La Jolla standard) and the SRM987 gave $^{87}Sr/^{86}Sr = 0{\cdot}710241 \pm 16$ (2 SD on 16 analyses).

ALMANDINE GARNETS

Petrography and classification

Almandine garnet occurs in a wide variety of volcanic rocks (andesites to rhyodacites) of the NPB and also in rare crustal xenoliths within the volcanic rocks. Garnet does not exceed 1–2 vol. % in abundance and is homogeneously distributed in each rock type. The garnets are dark red–violet and sometimes are surrounded by a thin light-coloured corona. They are usually 1–8 mm in diameter, but some may be as large as 2 cm. In general, garnets are larger in andesitic host rocks than in the more silicic ones.

The texture of the host rocks is variable, ranging from sparsely porphyritic trachytic to strongly porphyritic and medium grained. Plagioclase is the most common phenocryst coexisting with garnet. Hornblende and biotite occur also frequently and are together in the most silicic andesites and less silicic dacites. Biotite is the only mafic coexisting mineral in the rhyodacites but is absent from the andesites. Orthopyroxene occurs sporadically as a microphenocryst or groundmass phase, whereas clinopyroxene has never been observed. Mineral phases characteristic of many garnet-bearing S-type volcanic rocks worldwide, such as quartz, cordierite and K-feldspar, are absent from the NPB garnet-bearing volcanic rocks. On the basis of the petrographic characteristics of the garnets and their host rocks, the NPB almandines can be classified into five groups. Type 1A, Type 1B and Type 2 garnets are homogeneous or slightly zoned crystals with an inclusion assemblage similar to the mineral phases occurring in the host rocks. They appear to be primary igneous phases. Type 3 garnets are composite crystals having a light-coloured xenocrystic core and magmatic overgrowth. Type 4 garnets occur in crustal xenoliths. Details of petrographic and geochemical characters of the garnet types are given in Table 2.

Type 1A almandines (Fig. 2a and b) are 1–4 mm in size and occur in glassy rhyodacites (SiO_2 69–71 wt %)

Table 2: Summary of petrographic and geochemical features of garnet types from the NPB calc-alkaline volcanic rocks

	Type 1A	Type 1B	Type 2	Type 3	Type 4
Shape	euhedral to subhedral	subhedral to rounded	rounded	subhedral to rounded	rounded
Margin	sharp	sharp or partially resorbed	resorbed (zig-zag)	sharp	sharp
Reaction zone	no reaction zone	no reaction zone, or reaction corona of plag +am or +bi	reaction zone of plag	no reaction zone	no reaction zone
Inclusions	plag, ap, zr	plag, ap, bi, zr, ox	abundant plag, ap, ox	plag, ap, ox	qz
Coexisting phenocrysts	plag, bi	plag, am, bi, ±opx	plag, am, bi, ±opx	plag, am, bi	plag, bi, sill, ox, opx
Alm (mol %)	68–73	58–69	61–69	core: 71–85; rim: 55–66	57–63
CaO (wt %)	4·5–5·4	4·9–8·1	4·6–6·0	core: 0·8–1·6; rim: 4·2–8·1	0·8–2·7
MnO (wt %)	1·7–2·3	0·8–3·0	1·8–3·0	core: 0·7–7·1; rim: 0·8–2·7	3·3–10·9
Zoning (oxides in wt %)	no chemical zoning	CaO: 5·1–6·6 or 6·9–5·5; MgO: 4·1–6·1	CaO: 4·7–5·4 or 5·3–4·6; MgO: 3·9–5·0; MnO: 1·8–4·7	see above	CaO: 0·8–2·7; MgO: 2·8–7·5; MnO: 10·9–3·3
Eu/Eu*	0·17–0·20	0·27–0·35	0·67–0·68	0·14	n.d.
$\delta^{18}O$ (‰)	6·98–7·18	6·97–7·27	6·12–6·57	10·45	n.d.
Host rock	rhyodacite	dacite	andesite	andesite to dacite	xenolith in andesite
$(^{87}Sr/^{86}Sr)_{host\ rock}$	0·7092–0·7010	0·7099–0·7010	0·7068–0·7069	n.d.	n.d.

plag, plagioclase; ap, apatite; zr, zircon; bi, biotite; ox, ilmenite; am, hornblende; opx, orthopyroxene; sill, sillimanite; qz, quartz.

of the Visegrád Mts. They are euhedral to subhedral, but occasionally slightly rounded. Flow lines can be often observed around them (Fig. 2a). They are generally inclusion poor, the most common inclusions being plagioclase and needles of apatite. Intergrowth with plagioclase and/or biotite can be observed. Type 1B almandines (Fig. 2c and d) are the common garnets in silicic andesites and dacites (SiO_2 62–67 wt %) of the Börzsöny Mts. They are usually 2–5 mm in diameter, typically subhedral and often rounded (Fig. 2c). Intergrowths with plagioclase or biotite (Fig. 2c and d) and rarely with hornblende are characteristic. The almandines contain variable amounts of inclusions, mostly plagioclase, ilmenite and apatite. Type 2 garnets (Fig. 2e and f) occur in andesites (SiO_2 58–62 wt %) of Karancs and Breziny. They are usually 3–10 mm in diameter, but can reach 1·5 cm. They are always rounded and have resorbed, irregular margins. Inclusions are abundant and consist of mostly plagioclase, often in a concentric arrangement (Fig. 2f).

Composite garnets (Type 3; Fig. 2g and h) have been found in the Börzsöny Mts and in the Karancs (Fig. 1b). They are characterized by an irregular light-coloured core surrounded by a typical Type 1B or Type 2 outer garnet zone. Resorption between the light-coloured core garnet and the dark mantle garnet can often be observed. The core of some composite garnets has a distinct inclusion assemblage and/or contains xenoliths. Figure 2g shows an irregular-shaped crustal xenolith in the light-coloured core of a rounded garnet. This rock fragment consists of plagioclase, corundum, pleonaste (hercynite) and biotite. The garnet core includes further tiny fragments of this xenolith. A Type 3 garnet core from Šiatoroš (Fig. 1b) contains inclusions of biotite, ilmenite and orthopyroxene characterized by relatively high MnO content.

Crustal xenoliths are common within the garnet-bearing volcanic rocks from Šiatoroš and Breziny, but do not contain almandine. Almandine-bearing xenoliths occur rarely in the garnet-free volcanic rocks of the Börzsöny and Visegrád Mts. One of these samples consists of rounded garnets (Type 4; Fig. 2i) coexisting with plagioclase, biotite, sillimanite, pleonaste (hercynite) and orthopyroxene. The core of these garnets contains abundant quartz inclusions, but the outer zones are usually inclusion free.

Geochemistry of garnets

Major elements

Representative major element analyses of garnets from the NPB volcanic rocks are shown in Table 3. Comparisons of estimated Fe_2O_3 contents with values measured by Mössbauer spectrometry have revealed discrepancies particularly at low Fe_2O_3 content (e.g. Luth *et al.*, 1990). Measured Fe_2O_3 content of eight garnet samples by Mössbauer spectrometry (Kósa, 1998) was between 1·25 and 1·45 wt %, whereas the estimated Fe_2O_3 in the same samples was significantly lower (0·55–1·16 wt %). In this study, we used a stoichiometric method (Muhling & Griffin, 1991) for ferric ion estimation. End-member molecules were calculated based on the method of Muhling & Griffin (1991). All the published garnet analyses used for comparison in this study were re-calculated using the same scheme.

The petrographically distinguished garnet types have distinct chemical compositions illustrated in the Ca–Mg–Fe diagram (Fig. 3) and in Table 2. All of the NPB garnets have 58–73 mol % almandine component. Type 1A garnets show remarkably homogeneous chemistry, whereas Type 1B and Type 2 garnets are more variable. Rhyodacite-hosted Type 1A garnets have the highest almandine component, whereas Type 1B garnets from dacites and Type 2 garnets from andesites have lower almandine contents (Table 2). Among the minor components, pyrope is in the range of 9–14 mol % in Type 1A garnets, 13–23 mol % in Type 1B garnets and 12–21 mol % in Type 2 garnets. In contrast to the rough similarity between Type 1B and Type 2 garnets in terms of Mg–Fe abundance, there is a significant difference in the grossular and spessartine components. Overall, almandines from the NPB volcanic rocks have relatively high grossular (Gro >6 mol %) and low spessartine (Spe <10 mol %) contents. Type 1B garnets are the richest in Ca (Gro 10–18 mol %) and have generally low spessartine component (Spe <4 mol %). Andesite-hosted Type 2 garnets have typically lower grossular (Gro 6–13 mol %) and higher spessartine content (Spe 4–10 mol %). Type 1A garnets from the most silicic host rocks have similar grossular (Gro 8–12 mol %), but lower spessartine (Spe 3·5–4·5 mol %) components.

Single crystals are homogeneous or show slight zoning, whereas composite garnets (Type 3) have complex zoning patterns (Table 2). In Type 1A garnets a slight decrease of pyrope and slight increase of grossular from core to rim can be observed. Compositional trends in Type 1B garnets indicate increasing pyrope and increasing grossular from core to rim, whereas Type 2 garnets show mainly increasing pyrope and decreasing grossular and spessartine from core to rim.

Composite (Type 3) garnets have compositionally distinct cores with lower Ca contents (CaO <4 wt %, Gro <6·5 mol %; Fig. 3b) and higher Fe contents than the surrounding overgrowth. The MnO content of the cores is variable (0·5–6·5 wt %), but it is always higher than in the outer zone. The overgrowths show typical Type 1B or Type 2 compositions.

Type 4 garnet from the metamorphic xenolith is spessartine–almandine (60–64 mol % almandine, 18–25 mol % spessartine). Some of these garnets have a

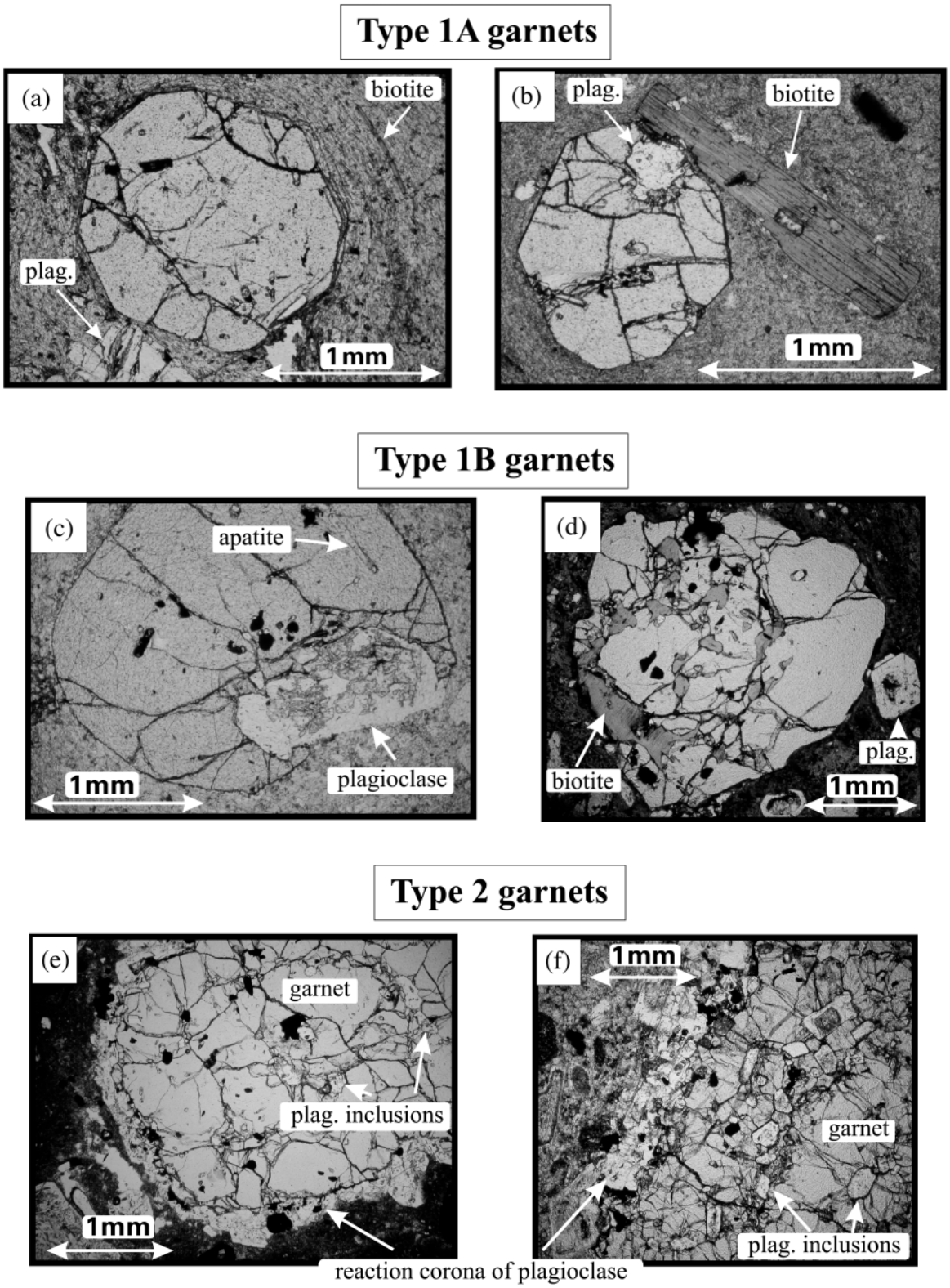
Type 1A garnets
(a)
biotite
plag.
1mm
(b)
plag.
biotite
1mm
Type 1B garnets
(c)
apatite
plagioclase
1mm
(d)
biotite
plag.
1mm
Type 2 garnets
(e)
garnet
plag. inclusions
1mm
(f)
1mm
garnet
plag. inclusions
reaction corona of plagioclase

Fig. 2.

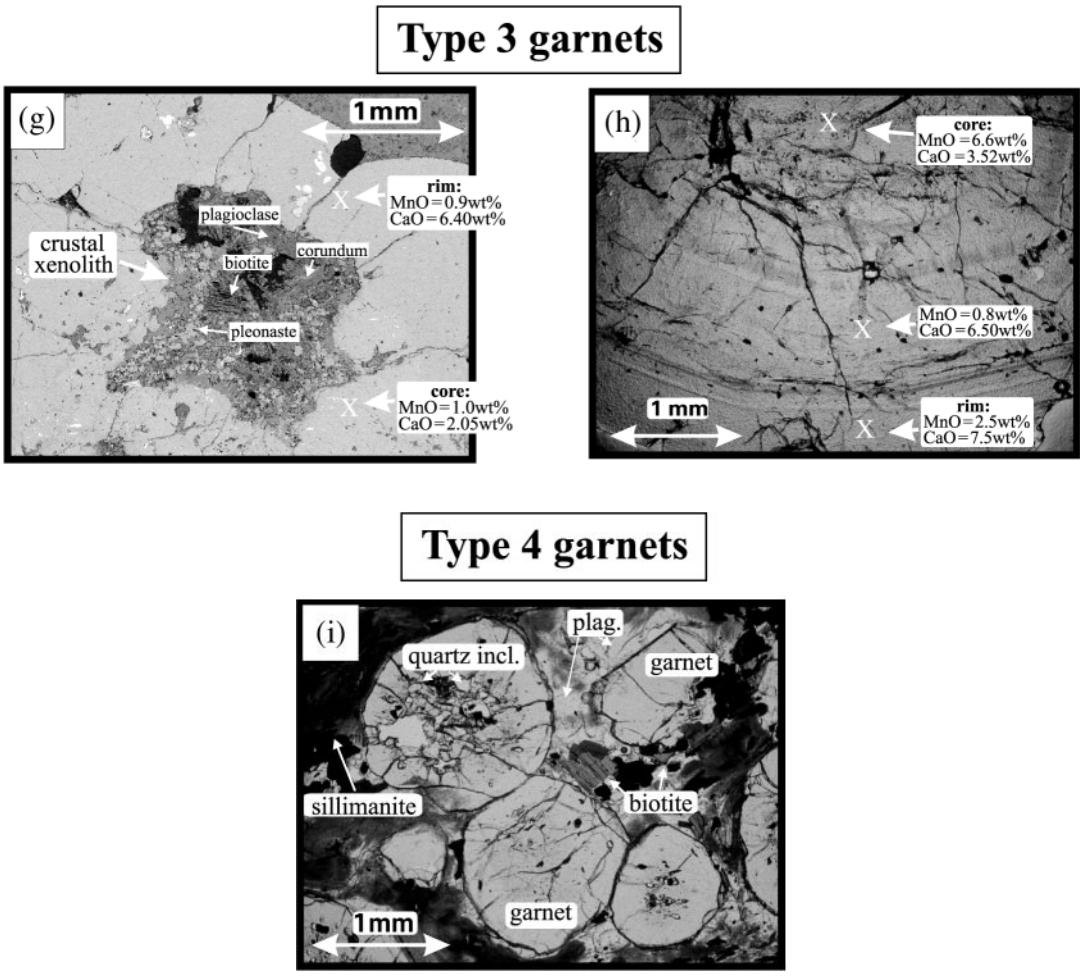

Fig. 2. Type 1A garnets: (a) euhedral garnet phenocryst in rhyodacite (sample ps6, Visegrád Mts); (b) euhedral garnet phenocryst intergrown with biotite and plagioclase in rhyodacite (sample x2, Visegrád Mts). Type 1B garnets: (c) rounded garnet phenocryst intergrown with plagioclase in dacite (sample B26; Börzsöny); (d) partially resorbed garnet phenocryst intergrown with biotite in dacite (sample b2l; Börzsöny). Type 2 garnets: (e) resorbed, rounded garnet phenocryst in andesite, containing numerous plagioclase inclusions and surrounded by a reaction corona of plagioclase (sample S-B1; Breziny, CSVF); (f) resorbed, rounded garnet phenocryst in andesite; this contains abundant plagioclase inclusions in a concentric arrangement and is surrounded by a reaction corona of plagioclase (sample kar1; Farkasnyak, Karancs). Composite (Type 3) garnets: (g) rounded garnet phenocryst in dacite. The low-Ca core contains crustal xenoliths composed of plagioclase, biotite, pleonaste (hercynite), corundum and quartz. The garnet overgrowth has a Type 1B character (sample l-nv; Börzsöny). (h) Detrital grain of zoned garnet. The light, high-Mn and low-Ca garnet core is surrounded by Type 1B rim (sample ver; Börzsöny). Type 4 garnet: (i) rounded garnets in a crustal xenolith embedded in andesite. The garnet cores have abundant quartz inclusions, but the outer zones are inclusion-free (sample csh4c, Visegrád Mts).

thin margin, in which Mn and Fe concentrations drastically decrease, whereas Mg and Ca increase.

Trace elements

Trace element compositions of selected garnets are presented in Table 4 and Fig. 4. They were determined by laser ablation ICP-MS analysing 2–4 points for each sample. The advantage of this method over the bulk garnet instrumental neutron activation analysis (INAA; e.g. Irving & Frey, 1978; Thirlwall & Fitton, 1983; Gilbert & Rogers, 1989) is that the influence of inclusions can be avoided, therefore it gives a better estimate of the trace element composition of garnets. However, we deliberately analysed a few garnet areas that contained inclusions such as plagioclase, apatite and zircon. These compositions enabled us to monitor and avoid the possible effect of these minerals on the garnet composition.

All the NPB garnets show strong light REE (LREE) depletion (Ce/Yb_N = 0·001–0·005) and have typical heavy REE (HREE) enriched patterns with variable HREE concentrations (Yb_N 59–850; Fig. 4). The degree of LREE depletion is more pronounced in these garnets than in previous INAA-derived results (Irving & Frey, 1978; Thirlwall & Fitton, 1983; Gilbert & Rogers, 1989). The garnet types previously distinguished by their petrographic characteristics have different trace element

Table 3: Representative major element composition of different garnet types in the NPB volcanic rocks

	Type 1A garnets								Type 1B garnets							
Locality:	Morgó hill (VM)		Holdvilág creek (VM)						Bajdázó quarry (BM)				Királyrét (BM)		Nagykő hill (BM)	
Sample:	ps4		x2		h1		cs5		B26				krb1		B5	
	core	rim	core	rim	core	rim	core	rim	core	rim	core	rim	core	rim	core	rim
SiO_2	36·74	37·09	37·17	37·01	37·21	37·37	37·57	37·78	37·71	37·89	37·60	37·87	37·41	37·74	38·26	38·28
TiO_2	0·18	0·25	0·30	0·24	0·35	0·31	0·36	0·19	0·34	0·41	0·48	0·42	0·24	0·33	0·40	0·47
Al_2O_3	20·25	20·68	20·67	20·43	20·92	21·10	21·11	21·26	20·98	21·35	21·01	21·05	20·87	20·93	21·58	21·65
FeO	32·60	32·92	32·06	32·21	31·99	31·84	32·15	32·67	28·54	28·05	29·78	29·23	29·78	29·21	27·92	26·44
MnO	1·81	1·65	2·09	1·92	2·32	1·82	2·43	2·20	0·90	0·80	1·06	0·69	1·87	0·83	1·14	1·01
MgO	2·40	2·29	3·37	3·21	3·33	3·35	3·18	2·97	4·10	4·75	4·05	4·70	3·77	4·74	5·54	6·12
CaO	5·33	5·17	4·69	4·87	4·66	4·86	4·69	4·34	6·92	7·33	7·06	6·89	6·18	6·58	6·22	6·37
Total	99·31	100·05	100·35	99·89	100·78	100·65	101·49	101·41	99·49	100·58	101·04	100·85	100·12	100·36	101·06	100·34
Cations based on 12 oxygens																
Si	2·9766	2·9818	2·9657	2·9694	2·9577	2·9676	2·9657	2·9862	2·9901	2·9625	2·9497	2·9613	2·9691	2·9660	2·9667	2·9718
Ti	0·0107	0·0149	0·0177	0·0144	0·0205	0·0181	0·0208	0·0109	0·0200	0·0239	0·0282	0·0244	0·0143	0·0193	0·0233	0·0270
Al	1·9337	1·9595	1·9435	1·9304	1·9594	1·9746	1·9642	1·9806	1·9601	1·9665	1·9423	1·9397	1·9514	1·9380	1·9722	1·9809
Fe^{3+}	0·0783	0·0433	0·0725	0·085	0·0619	0·0393	0·0488	0·0215	0·0295	0·0467	0·0791	0·0740	0·0646	0·0760	0·0374	0·0194
Fe^{2+}	2·1306	2·1703	2·0667	2·0763	2·0648	2·0753	2·0741	2·1382	1·8630	1·7873	1·8749	1·8376	1·9120	1·8438	1·7735	1·6974
Mn	0·1241	0·112	0·1409	0·1301	0·1557	0·1221	0·1622	0·1472	0·0600	0·0521	0·0702	0·0455	0·1254	0·0552	0·0745	0·0662
Mg	0·2896	0·2744	0·4003	0·3837	0·3945	0·3965	0·3738	0·3495	0·4845	0·5534	0·4733	0·5474	0·4458	0·5548	0·6403	0·7082
Ca	0·4625	0·4449	0·4007	0·4184	0·3959	0·4132	0·3966	0·3671	0·5874	0·6140	0·5930	0·5770	0·5255	0·5539	0·5168	0·5295
Mol fraction end-members																
X_{pyr}	0·0963	0·0914	0·1331	0·1275	0·1310	0·1319	0·1243	0·1164	0·1618	0·1840	0·1572	0·1820	0·1482	0·1845	0·2131	0·2360
X_{alm}	0·7086	0·7230	0·6869	0·6901	0·6858	0·6901	0·6898	0·7123	0·6221	0·5944	0·6226	0·6110	0·6355	0·6130	0·5902	0·5656
X_{gr}	0·1538	0·1482	0·1332	0·1391	0·1315	0·1374	0·1319	0·1223	0·1961	0·2042	0·1969	0·1919	0·1747	0·1842	0·1720	0·1764
X_{spess}	0·0413	0·0373	0·0468	0·0432	0·0517	0·0406	0·0539	0·0490	0·0200	0·0173	0·0233	0·0151	0·0417	0·0184	0·0248	0·0221

VM, Visegrád Mts.; BM, Börzsöny; CSVF, Central Slovakian Volcanic Field (Fig. 1b).

	Type 2 garnets									Type 4 garnets			
Locality:	Farkasnyak (Kar.)		Šiatoroš (Karancs)					Breziny (CSVF)		Nagy-Csikóvár (VM)			
Sample:	kar1		sat2					S-B1		csh4c			
	core	rim	core	rim	core	incl-rich zone	rim	core	rim	core	rim	core	rim
SiO_2	37·30	38·02	37·49	37·45	37·12	37·31	37·14	36·91	36·98	37·28	38·12	37·15	38·22
TiO_2	0·54	0·32	0·23	0·09	0·31	0·26	0·33	0·41	0·19	0·04	0·18		0·12
Al_2O_3	20·33	21·23	20·95	20·98	21·16	20·71	21·01	20·21	20·14	20·78	21·6	21·35	22·22
FeO	31·52	30·99	28·79	29·53	31·27	29·31	28·74	29·52	29·12	27·52	26·81	27·36	26·99
MnO	2·00	1·57	3·89	3·80	1·85	3·94	3·99	2·86	2·55	9·78	3·39	10·35	3·02
MgO	3·20	4·74	3·27	3·44	3·41	3·10	3·39	3·86	4·63	3·97	6·98	3·75	7·71
CaO	6·50	5·64	5·39	4·58	4·92	5·34	5·25	5·24	4·63	1·13	2·76	0·97	1·91
Total	101·39	102·51	100·01	99·87	100·04	99·97	99·85	99·01	98·24	100·5	99·84	100·93	100·19
Cations based on 12 oxygens													
Si	2·9459	2·9423	2·9883	2·9912	2·9627	2·9820	2·9669	2·9685	2·9827	2·9798	2·9813	2·9619	2·9671
Ti	0·0317	0·0186	0·0129	0·0052	0·0182	0·0153	0·0196	0·0246	0·0111	0·0024	0·0103		0·0070
Al	1·8918	1·9364	1·9676	1·9746	1·9904	1·9511	1·9776	1·9158	1·9145	1·9568	1·9906	2·0055	2·0330
Fe^{3+}	0·1296	0·1019	0·0309	0·0287	0·0284	0·0511	0·0355	0·0903	0·0910	0·0605	0·0173	0·0323	
Fe^{2+}	1·9525	1·9039	1·8883	1·9439	2·0590	1·9084	1·8845	1·8954	1·8734	1·7792	1·7362	1·7921	1·7523
Mn	0·1333	0·1027	0·2624	0·2567	0·1247	0·2665	0·2697	0·1947	0·1740	0·6613	0·2241	0·6990	0·1985
Mg	0·3763	0·5464	0·3884	0·4094	0·4052	0·3693	0·4032	0·4625	0·5564	0·4721	0·8134	0·4455	0·8921
Ca	0·5500	0·4673	0·4602	0·3916	0·4206	0·4572	0·4492	0·4514	0·3998	0·0965	0·2307	0·0824	0·1588
Mol fraction end-members													
X_{pyr}	0·1249	0·1809	0·1295	0·1364	0·1346	0·1230	0·1341	0·1540	0·1852	0·1569	0·2707	0·1476	0·2972
X_{alm}	0·6482	0·6304	0·6296	0·6476	0·6842	0·6358	0·6268	0·6310	0·6237	0·5913	0·5779	0·5936	0·5838
X_{gr}	0·1826	0·1547	0·1534	0·1305	0·1398	0·1523	0·1494	0·1503	0·1331	0·0321	0·0768	0·0273	0·0529
X_{spess}	0·0443	0·0340	0·0875	0·0855	0·0414	0·0888	0·0897	0·0648	0·0579	0·2198	0·0746	0·2315	0·0661

Table 3: continued

	Composite (Type 3) garnets													
Locality:	Verőce (BM)				Nógrád (BM)			Királyrét (BM)				Šiatoroš (Karancs)		
Sample:	ver				l-nv			krb1				sat1		
	core	zone1	zone2	rim	core	zone	rim	core1	core2	zone	rim	core1	core2	rim
SiO_2	36·74	37·67	38·10	37·22	36·96	38·06	38·17	36·74	37·13	37·32	37·40	37·33	38·12	37·77
TiO_2		0·42	0·47			0·33	0·27			0·52	0·19			0·18
Al_2O_3	20·58	20·92	21·33	20·74	21·43	21·65	21·74	20·71	20·97	20·93	21·02	21·64	22·14	21·26
FeO	32·51	30·94	26·53	34·84	34·61	28·20	28·24	34·08	34·07	26·32	29·44	30·52	26·99	29·42
MnO	6·32	1·74	0·81	3·15	1·18	0·92	0·92	3·09	2·03	1·08	2·36	4·23	7·09	2·46
MgO	1·18	4·23	5·66	1·99	3·47	4·28	4·70	3·78	4·31	5·28	3·44	4·74	6·37	4·19
CaO	3·60	5·28	8·12	3·37	1·74	7·06	6·32	1·17	1·28	7·57	6·55	1·67	0·89	5·48
Total	100·93	101·20	101·02	101·31	99·39	100·50	100·36	99·57	99·79	99·02	100·40	100·13	101·60	100·76
Cations based on 12 oxygens														
Si	2·9703	2·9593	2·9474	2·9801	2·9809	2·9815	2·9868	2·9700	2·9789	2·9515	2·9650	2·9688	2·9613	2·9726
Ti		0·0245	0·0269			0·0192	0·0158			0·0308	0·0109			0·0104
Al	1·9607	1·9363	1·9439	1·9572	2·0370	1·9986	2·0049	1·9732	1·9824	1·9502	1·9636	2·0283	2·0268	1·9720
Fe^{3+}	0·0685	0·0792	0·0811	0·0621		0·0007		0·0562	0·0384	0·0669	0·0600	0·0026	0·0113	0·0446
Fe^{2+}	2·1297	1·9535	1·6352	2·2709	2·3344	1·8469	1·8480	2·2479	2·2476	1·6738	1·8919	2·0275	1·7421	1·8917
Mn	0·4323	0·1156	0·0529	0·2136	0·0806	0·0607	0·0609	0·2113	0·1378	0·0722	0·1581	0·2848	0·4663	0·1636
Mg	0·1418	0·4951	0·6526	0·2372	0·4171	0·4994	0·5481	0·4551	0·5153	0·6220	0·4063	0·5615	0·7375	0·4913
Ca	0·3114	0·4442	0·6726	0·2886	0·1503	0·5921	0·5298	0·1010	0·1099	0·6410	0·5559	0·1419	0·0737	0·4620
Mol fraction end-members														
X_{pyr}	0·0470	0·1646	0·2166	0·0788	0·1399	0·1665	0·1835	0·1509	0·1712	0·2067	0·1349	0·1862	0·2442	0·1633
X_{alm}	0·7063	0·6493	0·5427	0·7544	0·7827	0·6158	0·6187	0·7455	0·7466	0·5563	0·6281	0·6723	0·5769	0·6288
X_{gr}	0·1033	0·1477	0·2232	0·0959	0·0504	0·1974	0·1774	0·0335	0·0365	0·2130	0·1845	0·0471	0·0244	0·1536
X_{spess}	0·1434	0·0384	0·0176	0·0710	0·0270	0·0202	0·0204	0·0701	0·0458	0·0240	0·0525	0·0944	0·1544	0·0544

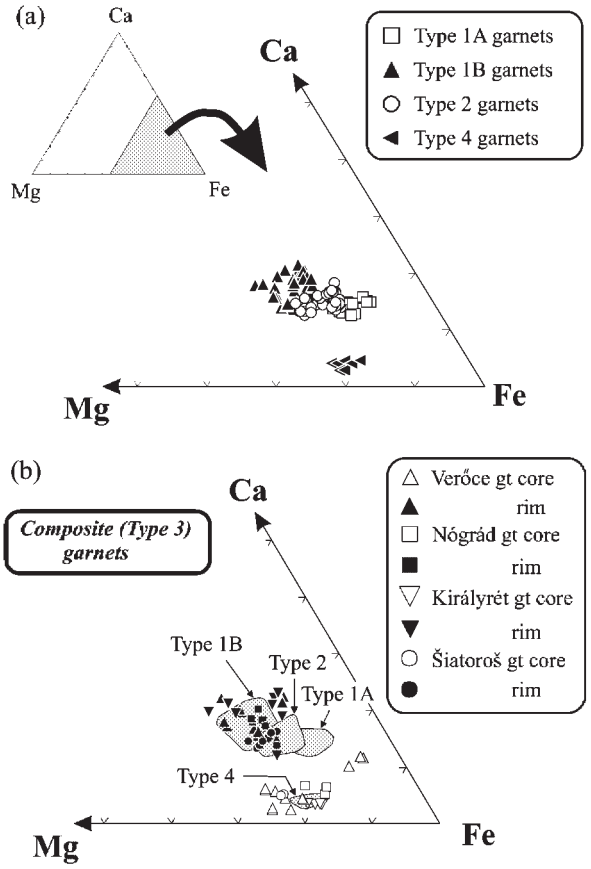

Fig. 3. Variation of chemical composition of the different garnet types illustrated in the Mg–Ca–Fe diagram. (a) primary (Type 1A, 1B and 2) and Type 4 garnets; (b) cores and rims of composite (Type 3) garnets.

compositions and different REE profiles. The total REE content and the Y, Zr, Hf, Th and U concentrations increase from Type 2 garnet through Type 1B to Type 1A garnets. Furthermore, the negative Eu anomaly tends to be stronger towards the Type 1A garnets (Table 2, Fig. 4). The core of the composite garnet (Type 3) from Verőce (Börzsöny Mts) has lower Y and higher Zr, Hf concentrations than the primary garnets (Table 4) and shows a different REE pattern.

Oxygen isotopes

Although $\delta^{18}O$ values have been reported for metamorphic almandines (e.g. Taylor & Coleman, 1968; Kohn *et al.*, 1997), our results are the first published data for igneous almandines since the single analysis of Mason *et al.* (1996). A large amount of laser fluorination oxygen isotope data for mineral phases from Neogene volcanic rocks of the Carpathian–Pannonian region has already been published (Downes *et al.*, 1995; Mason *et al.*, 1996; Dobosi *et al.*, 1998). The samples were analysed in the same laboratory (RHUL) using the same technique (Mattey & Macpherson, 1993); therefore these data provide a comparative dataset.

Values of $\delta^{18}O$ for the NPB garnets show a wide range from 6·1 to 10·5‰ (Table 5). Type 2 garnets have the lowest $\delta^{18}O$ values (6·1 and 6·6‰), whereas values for Type 1A and Type 1B garnets are slightly higher but show a narrow range (6·9–7·3‰). Two composite garnets have elevated $\delta^{18}O$ values (8·0 and 10·5, respectively). Garnet in an andesite from the East Carpathians (Mason *et al.*, 1996) has a slightly higher $\delta^{18}O$ value (7·3‰) than most of the Type 1A and 1B garnets. The oxygen isotope data for igneous garnets from the NPB do not correlate with the major element compositions of garnets, but correlate well with the host rock $^{87}Sr/^{86}Sr$ (Fig. 5) and $^{143}Nd/^{144}Nd$ values. $\delta^{18}O$ values of composite garnets are between the typical values of igneous almandines published in this study and metamorphic ones (11·4–13·4‰; Kohn *et al.*, 1997), consistent with the assumption that both the xenocrystic core and igneous overgrowth of the composite garnet were analysed. Whole-rock data for garnet-bearing volcanic rocks from SE Spain and the Lesser Antilles (Table 1) show strongly elevated $\delta^{18}O$ values (13·1–15·6‰; Munksgaard, 1984; Davidson & Harmon, 1989). As whole-rock oxygen isotope data are usually higher than the included minerals by at least 1‰, garnets from these rocks could have higher $\delta^{18}O$ values than the NPB garnets. Garnets from the English Lake District (Table 1) have $\delta^{18}O$ values of 8·4–8·6‰ (M. F. Thirlwall, unpublished data, 1999), higher than those for the igneous garnets from the NPB.

The oxygen isotope data of the NPB garnets are higher than the typical $\delta^{18}O$ values inferred for the asthenospheric mantle beneath the Pannonian Basin (5·0–5·4‰; Dobosi *et al.*, 1998), but $\delta^{18}O$ values of Type 2 garnets are close to the values of the lithospheric mantle as shown by separated minerals of ultramafic xenoliths from the East Carpathians ($\delta^{18}O$ = 5·4–5·9‰; Mason, 1995; Fig. 5).

Mafic minerals from the host volcanic rocks show roughly similar $\delta^{18}O$ values to the garnets, although some biotites have higher $\delta^{18}O$ values. Comparing the oxygen isotope data for the garnets with data for the mafic minerals (pyroxenes, hornblende) of the garnet-free volcanic rocks from the same area (Downes *et al.*, 1995), only some amphiboles show lower $\delta^{18}O$ values (Fig. 5). In general, almandine garnets from the NPB have the lowest $\delta^{18}O$ values at a given host rock $^{87}Sr/^{86}Sr$ value among the calc-alkaline volcanic suite of the Carpathian–Pannonian region.

Inclusions and coexisting minerals

Hornblende is a common mafic phenocryst phase in the andesites and dacites, being intergrown with garnet in

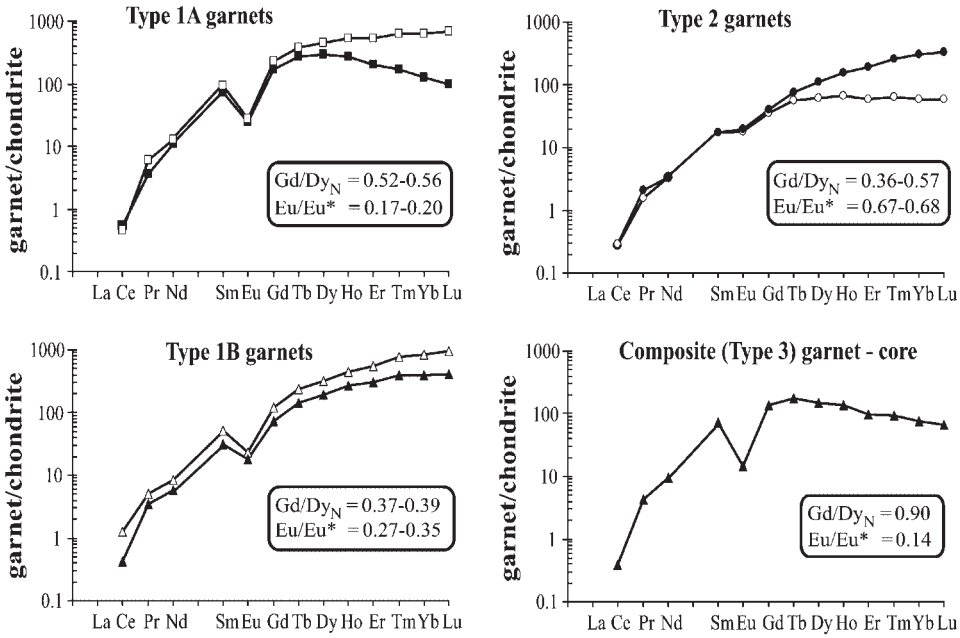

Fig. 4. Chondrite (Nakamura, 1974) normalized REE patterns of the different garnet types from the NPB.

Table 4: Trace element composition of selected NPB garnets by laser ablation ICP-MS

Locality:	Morgó hill (VM)	Dömös (VM)	Csódi hill (VM)	Kóspallag (BM)	Šiatoroš (Karancs)	Breziny (CSVF)	Verőce (BM)
Sample:	ps4	l2	csh	kp	sat	SB-1	ver—core
Type:	Type 1A	Type 1A	Type 1B	Type 1B	Type 2	Type 2	Type 3
Sr	0·62	0·225	0·58	0·3	0·323	0·24	0·42
Y	1073	585	911	568	151	345	277
Zr	84	89	74	36	61	69	178
La		0·026	0·63	0·036	0·009		
Ce	0·4	0·47	1·1	0·37	0·240	0·25	0·33
Pr	0·67	0·405	0·58	0·39	0·177	0·23	0·485
Nd	8·1	6·85	5·4	3·6	2·133	2·1	6
Sm	19·4	14·75	10·7	6·4	3·567	3·5	14·7
Eu	2·1	1·85	1·8	1·4	1·367	1·5	1·105
Gd	64	46	34	20	9·700	11	37·5
Tb	18	12·75	11·1	6·6	2·633	3·6	8·3
Dy	153	102	109	67	21·333	38	51·5
Ho	37	19	32	19	4·667	11	9·5
Er	117	44·5	124	69	13·333	43	22
Tm	19	5·1	23	12	1·900	7·8	2·8
Yb	140	27·5	187	86	13·000	66	16·5
Lu	23	3·25	33	14	1·967	11·4	2·3
Hf	1·7	1·51	1·2	0·71	0·773	0·93	2·75
Ta	0·17	0·093	0·11	0·078	0·019	0·05	0·068
Th	0·053	0·0085	0·068	0·007	0·004	0·004	0·006
U	0·076	0·127	0·029	0·027	0·025	0·015	0·057

Table 5: $\delta^{18}O$ values of selected garnets (duplicate results are also shown) and coexisting mafic minerals by laser fluorination

Sample	Locality	Mineral	$\delta^{18}O$ (‰)
ps4	Morgó hill (VM)	garnet (Type 1A)	7·18
		biotite	7·58
l2	Dömös (VM)	garnet (Type 1A)	6·98
csh	Csódi hill (VM)	garnet (Type 1B)	6·97
			6·96
		amphibole	7·07
B26	Bajdázó (BM)	garnet (Type 1B)	7·26
		biotite	7·49
l-nv	Castle hill, Nógrád	garnet (Type 1B)	7·29
	(BM)		7·26
		biotite	8·42
sat	Šiatoroš (Karancs)	garnet (Type 2)	6·12
S-B1	Breziny (CSVF)	garnet (Type 2)	6·57
			6·60
KP	Kóspallag (BM)	garnet (Type 3)	8·00
VER	Verőce (BM)	garnet (Type 3)	10·45
			10·50

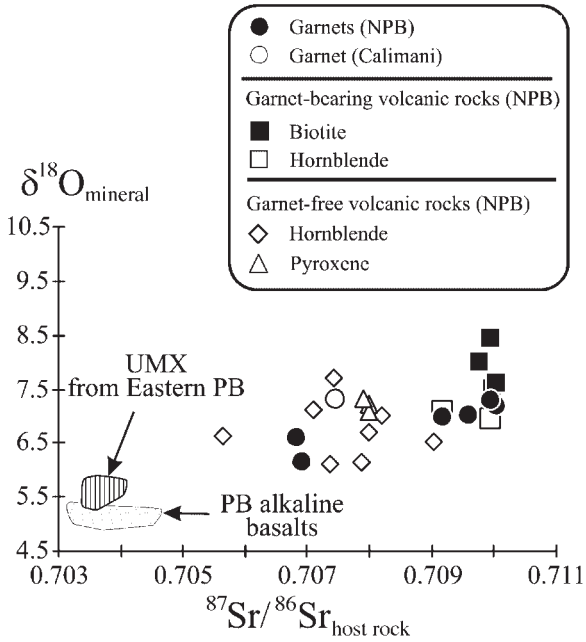

Fig. 5. $\delta^{18}O_{mineral}$ vs $(^{87}Sr/^{86}Sr)_{host\ rock}$ plot for the NPB garnets and other mafic minerals (hornblende, biotite and pyroxene) from garnet-bearing and garnet-free volcanic rocks of the NPB (data are from this study; Downes *et al.*, 1995; A. Demény & Sz. Harangi, unpublished data, 1999). For comparison, garnet from the Calimani Mts, Eastern Carpathians (Mason *et al.*, 1996) and the fields of the Neogene alkali basalts (based on olivine phenocrysts) of the Pannonian Basin (PB; Dobosi *et al.*, 1998) and the ultramafic xenoliths (UMX; based on olivine and clinopyroxene) of the eastern Pannonian Basin (Mason, 1995) are also shown.

some samples. It shows variable resorption and formation of opacite rims. Hornblende compositions (Table 6) are tschermakite, magnesiohastingsite and pargasite based on the IMA nomenclature (Leake *et al.*, 1997). Amphiboles intergrown with garnets have similar compositions to the phenocrysts. In general, there are positive correlations between Al^{iv} and Ti, and Al^{iv} and Na + K (Fig. 6), corresponding to crystallization under falling temperature and pressure (Gill, 1981; Green, 1992). Most amphiboles in the garnet-bearing volcanic rocks show higher Al^{iv}, Ti and Na + K values than amphiboles of the garnet-free volcanic rocks and approach the values of the magnesio-hastingsites occurring in mafic cognate xenoliths from the NPB (Sz. Harangi, unpublished data, 1998).

Biotite occurs in variable amounts in the garnet-bearing volcanic rocks of the NPB and is less common in the garnet-free varieties. The intergrowth and coexistence of biotite and garnet suggest contemporaneous crystallization. Biotite has distinct chemical compositions (Table 7) in the different rock types, illustrating compositional dependence on the nature of host magma (Abdel-Rahman, 1994). They are less magnesian (*mg*-number 0·29–0·40) and less potassic (K_2O 8·1–8·7 wt %) in rhyodacites compared with micas in dacites and andesites (*mg*-number 0·45–0·53, K_2O 8·5–9·4 wt %). The garnet–biotite Mg–Fe distribution coefficient, i.e. $(Mg/Fe)^{gt}/(Mg/Fe)^{bi}$, varies between 0·24 and 0·35. These values are higher than the Mg–Fe distribution coefficient typical of metamorphic garnet–biotite pairs (0·09–0·20; Lyons & Morse, 1970) but match that of the garnet–biotite pairs from igneous rocks (0·24–0·32; Lyons & Morse, 1970). The chemical composition of biotite in the garnet-bearing crustal xenolith is very different, having higher TiO_2 (5·3 wt %) and MnO (0·74 wt %) contents.

Plagioclase (Table 8) is the most common mineral in the garnet-bearing volcanic rocks of the NPB, occurring as phenocrysts, intergrowths with garnet (Fig. 2c), inclusions in mafic minerals and reaction coronas around garnet (Fig. 2e and f). The phenocrysts show normal, reverse and oscillatory zoning ($An_{41–88}$). Plagioclase inclusions in garnet show the same chemical variation as the phenocrysts in each sample ($An_{55–91}$; Fig. 7). Most of them are more calcic than the plagioclase inclusions in biotite and amphibole phenocrysts ($An_{53–78}$).

Ilmenite is a common minor inclusion in Type 1B and Type 2 garnets and occurs also as rare microphenocrysts. No ilmenite has been found in Type 1A garnets. Its composition (Table 9) differs in the two garnet types, with more TiO_2 and less MnO in Type 1B garnets. Ilmenite in a xenocrystic core of a Type 3 composite

Table 6: Representative chemical composition of amphiboles coexisting with garnets

Locality:	Bajdázó quarry (BM)			Nógrád	Királyrét (BM)		Nagykő hill (BM)			Šiatoroš (Karancs)		Breziny (CSVF)	
Sample:	b26			l-nv	krb1		b5b			sat1		S-B1	
Type:	phcr coex gt	phcr core	phcr rim	relict mphcr	phcr core	phcr rim	phcr core	phcr rim	incl in gt	mphcr core	mphcr rim	phcr	phcr
SiO_2	40·01	40·58	40·57	41·26	42·94	43·04	43·34	42·60	41·31	42·49	41·78	41·52	41·63
TiO_2	2·65	1·77	2·53	2·35	1·26	1·19	1·39	1·57	2·19	1·52	1·44	2·07	1·17
Al_2O_3	15·98	15·57	15·68	16·17	12·94	13·13	13·27	12·82	14·65	12·41	12·44	13·85	12·07
FeO	13·87	16·31	15·12	13·73	17·30	19·47	17·87	18·54	16·18	19·91	17·46	15·64	21·26
MnO	0·15	0·18	0·06	0·10		0·17	0·24	0·15	0·21	0·32	0·27	0·24	0·44
MgO	10·83	9·70	10·65	11·12	10·36	9·10	10·39	10·15	10·40	9·53	10·63	10·62	9·71
CaO	10·51	10·89	10·69	11·40	10·64	10·35	9·56	8·92	10·45	9·68	9·55	10·76	9·44
Na_2O	2·00	1·91	1·85	2·08	1·70	1·64	1·93	1·93	1·93	2·13	2·54	2·22	1·94
K_2O	0·93	0·93	0·96	0·86	0·56	0·55	0·50	0·45	0·61	0·45	0·46	0·67	0·51
Total	96·93	97·84	98·11	99·07	97·70	98·64	98·49	97·13	97·93	98·44	96·57	97·59	98·17
Cations based on 22 oxygens													
Si	5·864	5·960	5·892	5·945	6·269	6·259	6·215	6·177	6·005	6·180	6·158	6·098	6·056
Al^{iv}	2·136	2·040	2·108	2·055	1·731	1·741	1·785	1·823	1·995	1·820	1·842	1·902	1·944
Al^{vi}	0·624	0·655	0·576	0·691	0·495	0·509	0·458	0·368	0·515	0·307	0·319	0·495	0·125
Ti	0·292	0·195	0·276	0·255	0·138	0·130	0·150	0·171	0·239	0·166	0·160	0·229	0·128
Fe^{3+}	0·885	0·847	0·955	0·595	1·045	1·182	1·462	1·714	1·089	1·479	1·374	0·804	1·976
Mg	2·366	2·123	2·305	2·388	2·254	1·972	2·221	2·194	2·253	2·066	2·335	2·325	2·105
Fe^{2+}	0·815	1·156	0·881	1·059	1·067	1·186	0·681	0·535	0·878	0·943	0·778	1·117	0·610
Mn	0·018	0·022	0·007	0·012		0·021	0·028	0·018	0·026	0·039	0·034	0·030	0·054
Ca	1·650	1·714	1·663	1·760	1·664	1·612	1·469	1·386	1·627	1·508	1·508	1·693	1·471
Na^{B}	0·349	0·286	0·337	0·240	0·336	0·388	0·530	0·543	0·373	0·492	0·492	0·307	0·529
Na^{A}	0·219	0·258	0·184	0·341	0·145	0·074	0·007		0·171	0·109	0·234	0·325	0·018
K	0·174	0·174	0·178	0·158	0·104	0·102	0·091	0·083	0·113	0·083	0·086	0·125	0·095
mg-no.	0·74	0·65	0·72	0·69	0·68	0·62	0·77	0·80	0·72	0·69	0·75	0·68	0·78

phcr, phenocryst; mphcr, microphenocryst; gt, garnet; incl, inclusion; coex, coexisting with.

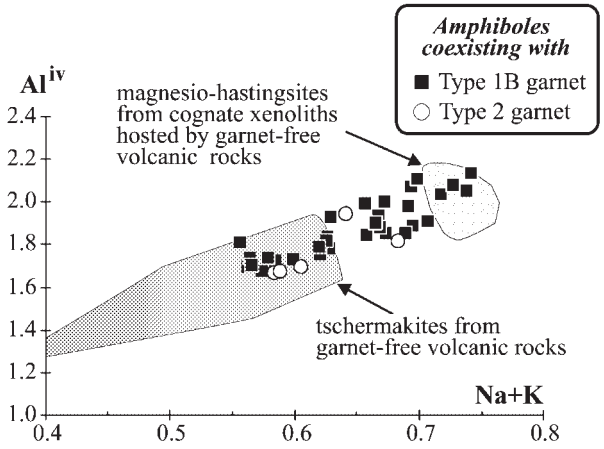

Fig. 6. Amphiboles coexisting with Type 1B and Type 2 garnets show positive correlations in the Al^{iv} vs Na + K diagram. This trend indicates crystallization under falling temperature and pressure. Amphiboles with the highest Al^{iv} and alkali content overlap the field of magnesio-hastingsites occurring in mafic cognate xenoliths, which are thought to consist of high-pressure mineral phases (amphiboles from garnet-free volcanic rocks: Sz. Harangi, unpublished data, 1998).

garnet from the Karancs Mts contains significantly higher MnO (MnO 1·9–2·1 wt %).

Orthopyroxene microphenocrysts are magnesian ferrosilite ($En_{44–51}Wo_{1·4}Fs_{47–54}$). Orthopyroxene inclusions in garnet cores of the Karancs andesite contain relatively high MnO (MnO 2·3–5·9 wt %) coinciding with the higher MnO content of the garnet core (MnO >3·7 wt %) and the coexisting inclusion phases.

GEOCHEMISTRY OF GARNET-BEARING VOLCANIC ROCKS

The garnet-bearing volcanic rocks in the NPB range in composition from andesites to rhyodacites (SiO_2 58·2–70·1 wt %; Table 10). They show a continuous trend from medium- to high-K calc-alkaline volcanic rocks (Fig. 8) and are usually more silicic than the garnet-free volcanic rocks in the same region. Garnet-bearing rhyodacites are slightly peraluminous, having normative corundum in the CIPW composition (c = 1·5–2·1) and A/CNK ratio [Al_2O_3/(CaO + Na_2O + K_2O) ratio in molar proportions] >1 (A/CNK = 1·07–1·12). Dacites containing Type 1B garnets are both peraluminous and metaluminous (c = 0–1·9, di = 0–1·7; A/CNK = 0·95–1·09), whereas Type 2 garnet-bearing andesites are diopside-normative (di = 0·6–1·6; A/CNK = 0·94–0·96).

Trace element compositions of the garnet-bearing volcanic rocks (Table 10) are similar to those of the garnet-free varieties. They show relative enrichment of large ion lithophile elements (LILE), negative Nb anomalies and positive Pb anomalies in a mid-ocean ridge basalt (MORB)-normalized plot (Fig. 9), typical of subduction-related magmas. The REE show similar patterns to the garnet-free rocks in the range of La–Eu; however, the garnet-bearing rocks are relatively depleted in the HREE (Fig. 10). This HREE depletion is most pronounced in Type 1A and most Type 1B garnet-bearing dacites and rhyodacites. Similar strong HREE depletion was recognized in the garnet-bearing rhyolites from the Pyrenees (Gilbert & Rogers, 1989), whereas the English Lake District andesites and dacites (Thirlwall & Fitton, 1983) and several other garnet-bearing volcanic rocks worldwide (Irving & Frey, 1978) do not show this feature. The NPB andesites containing Type 2 garnets show no HREE depletion (Fig. 10). In general, the garnet-bearing volcanic rocks of the NPB do not show a significant negative Eu anomaly, in contrast to garnet-bearing dacites and rhyolites worldwide (e.g. Pyrenees, English Lake District, Japan, Victoria; Eu/Eu* = 0·32–0·74). The Eu/Eu* ratio varies between 0·76 and 0·97 in the NPB rocks, but most of them are in a narrow range from 0·87 to 0·97. These values are usually even higher than the Eu/Eu* ratios of the garnet-free volcanic rocks of the NPB at given La_N.

Initial $^{87}Sr/^{86}Sr$ and $^{143}Nd/^{144}Nd$ ratios in the garnet-bearing volcanic rocks of the NPB vary widely ($^{87}Sr/^{86}Sr$ = 0·7062–0·7100; $^{143}Nd/^{144}Nd$ = 0·51230–0·51246; Table 10) and reach the highest $^{87}Sr/^{86}Sr$ and lowest $^{143}Nd/^{144}Nd$ values among the calc-alkaline volcanic rocks in this area. The dacites and rhyodacites have fairly similar radiogenic isotope compositions ($^{87}Sr/^{86}Sr$ = 0·7090–0·7100; $^{143}Nd/^{144}Nd$ = 0·51235–0·51246) and differ significantly from the garnet-bearing andesites ($^{87}Sr/^{86}Sr$ = 0·7062–0·7069; $^{143}Nd/^{144}Nd$ = 0·51244–0·51246).

DISCUSSION

Origin of almandine garnets in the NPB volcanic rocks

Almandine garnets in volcanic rocks can be (1) primary magmatic phases or (2) xenocrysts derived either from disaggregated country rocks or represent a restite phase. The petrographic and geochemical characteristics of Type 1A, 1B and Type 2 almandines in the NPB volcanic rocks suggest that they are primary igneous phases cognate with their host rocks. Garnets are commonly intergrown with phenocrysts and contain an inclusion assemblage akin to the phenocrysts of the host rocks. Furthermore, plagioclase inclusions in the garnets and plagioclase phenocryst cores have identical compositions in each sample.

Garnets in the NPB andesites are usually surrounded by a reaction corona of plagioclase ± biotite or amphibole,

Table 7: Representative chemical composition of biotite coexisting with garnets

Locality:	Holdvilág creek (VM)				Csódi hill (VM)		Bajdázó quarry (BM)			Nagykő hill (BM)		Királyrét (BM)		Šiatoroš (Karancs)	
Sample:	h1		x2		csh		B26			b2l		krb1		sat2	
Type:	phcr	phcr	phcr	phcr coex gt	phcr	incl in gt	phcr	mica intgr gt	mica intgr gt	mica intgr gt	phcr	phcr	incl in gt	phcr in cum group	incl in gt
SiO_2	34·59	34·66	34·52	34·39	37·05	36·12	36·73	35·01	35·63	36·22	37·32	36·01	35·66	35·15	36·29
TiO_2	3·90	3·60	4·09	4·18	4·01	4·23	4·21	4·59	4·85	4·12	3·71	3·92	4·33	4·04	4·05
Al_2O_3	16·56	16·04	16·02	15·94	17·54	17·18	17·26	15·32	15·57	16·07	17·14	15·63	15·30	15·09	15·84
FeO	24·93	24·81	25·51	25·14	12·48	16·50	18·81	19·43	19·62	20·19	18·93	20·87	20·35	22·25	18·64
MnO	0·09	0·15	0·09		0·20						0·07			0·14	0·32
MgO	7·75	7·84	7·97	7·90	16·36	13·06	11·48	10·99	11·39	10·69	9·67	10·93	11·09	9·53	12·24
CaO	0·10	0·11						0·08	0·12		0·09		0·08		0·21
Na_2O	0·86	0·74	1·07	0·99	1·05	0·74	0·82	0·74	0·95	1·12	0·39	0·92	0·97	1·14	0·90
K_2O	7·91	8·12	8·27	8·46	9·30	9·39	9·31	9·03	8·96	8·94	8·11	8·60	8·49	8·79	8·94
Total	96·69	96·07	97·54	97·00	97·99	97·22	98·62	95·19	97·09	97·35	95·43	96·88	96·27	96·13	97·43
Cations based on 22 oxygens															
Si	5·3295	5·3824	5·3065	5·3129	5·3246	5·3351	5·3913	5·3786	5·3604	5·4335	5·6054	5·4384	5·4153	5·4192	5·4099
Al^{iv}	2·6705	2·6176	2·6935	2·6871	2·6754	2·6649	2·6087	2·6214	2·6396	2·5665	2·3946	2·5616	2·5847	2·5808	2·5901
Al^{vi}	0·3367	0·3181	0·2089	0·2152	0·2955	0·3258	0·3772	0·1525	0·1212	0·2747	0·6395	0·2204	0·1536	0·1611	0·1929
Ti	0·4518	0·4204	0·4728	0·4856	0·4333	0·4698	0·4647	0·5302	0·5487	0·4647	0·4190	0·4452	0·4944	0·4684	0·4540
Al	3·0072	2·9357	2·9024	2·9023	2·9709	2·9907	2·9859	2·7739	2·7608	2·8412	3·0341	2·7820	2·7383	2·7419	2·7830
Fe^{2+}	3·2123	3·2221	3·2795	3·2481	1·4999	2·0381	2·3090	2·4963	2·4685	2·5329	2·3778	2·6359	2·5844	2·8688	2·3238
Mn	0·0117	0·0197	0·0117		0·0243						0·0089			0·0182	0·0404
Mg	1·7798	1·8147	1·8261	1·8191	3·5044	2·8752	2·5116	2·5166	2·5541	2·3902	2·1648	2·4604	2·5102	2·1899	2·7196
Ca	0·0165	0·0183						0·0131	0·0193		0·0144		0·0130		0·0335
Na	0·2569	0·2228	0·3189	0·2965	0·2925	0·2119	0·2333	0·2204	0·2771	0·3257	0·1135	0·2693	0·2856	0·3407	0·2601
K	1·5547	1·6085	1·6217	1·6672	1·7049	1·7692	1·7432	1·7696	1·7195	1·7107	1·5538	1·6568	1·6446	1·7287	1·7000
mg-no.	35·65	36·02	35·77	35·89	70·03	58·52	52·1	50·20	50·86	48·54	47·66	48·28	49·27	43·30	53·93

intgr, intergrown with (for further abbreviations, see Table 6).

Table 8: Representative chemical composition of plagioclases coexisting with garnets (for abbreviations see Table 6)

Locality:	Holdvilág creek (VM)		Morgó hill (VM)			Bajdázó quarry (BM)					Breziny (CSVF)			
Sample:	h1		ps4			B26					SB-1			
Type:	incl in gt	phcr	incl in gt	phcr core	phcr rim	phcr coex gt	incl in gt	incl in mica	phcr core	phcr rim	incl in gt	incl in gt	phcr core	phcr rim
SiO_2	49·27	47·36	52·64	51·34	54·35	46·14	47·66	52·14	45·73	53·51	46·90	51·14	51·08	53·21
Al_2O_3	33·45	32·71	31·53	30·65	28·91	34·47	33·31	30·58	34·48	29·32	32·92	30·31	30·59	29·38
FeO	0·32		0·27		0·19		0·40	0·24	0·12	0·20	0·28	0·42	0·32	0·27
CaO	15·11	17·03	12·87	14·39	11·93	19·00	15·45	13·95	18·94	12·53	17·27	13·93	14·19	12·46
Na_2O	2·35	2·21	3·40	3·89	5·08	1·44	2·07	4·11	1·38	4·83	2·21	3·93	3·83	4·72
K_2O	0·07		0·12	0·14	0·15			0·11				0·13	0·09	0·17
Total	100·57	99·31	100·83	100·41	100·61	101·05	98·89	101·13	100·65	100·39	99·58	99·86	100·10	100·21
Cations based on 8 oxygens														
Si	2·2337	2·1908	2·3604	2·3317	2·4458	2·1095	2·2026	2·3494	2·1007	2·4167	2·1703	2·3373	2·3286	2·4101
Al	1·7873	1·7833	1·6663	1·6406	1·5333	1·8574	1·8143	1·6239	1·8668	1·5607	1·7954	1·6327	1·6436	1·5684
Fe	0·0121		0·0101		0·0071		0·0154	0·0090	0·0046	0·0075	0·0108	0·0160	0·0122	0·0102
Ca	0·7339	0·8440	0·6183	0·7002	0·5752	0·9307	0·7650	0·6734	0·9322	0·6063	0·8562	0·6821	0·6931	0·6046
Na	0·2065	0·1982	0·2955	0·3425	0·4432	0·1276	0·1854	0·3590	0·1229	0·4229	0·1982	0·3482	0·3385	0·4145
K	0·0040		0·0068	0·0081	0·0086			0·0063				0·0075	0·0052	0·0098
Mole fraction end-members														
Or	0·42		0·74	0·77	0·84			0·61				0·72	0·50	0·95
Ab	21·87	19·02	32·10	32·59	43·15	12·06	19·51	34·56	11·65	41·09	18·80	33·55	32·65	40·29
An	77·71	80·98	67·16	66·63	56·01	87·94	80·49	64·83	88·35	58·91	81·20	65·73	66·85	58·76

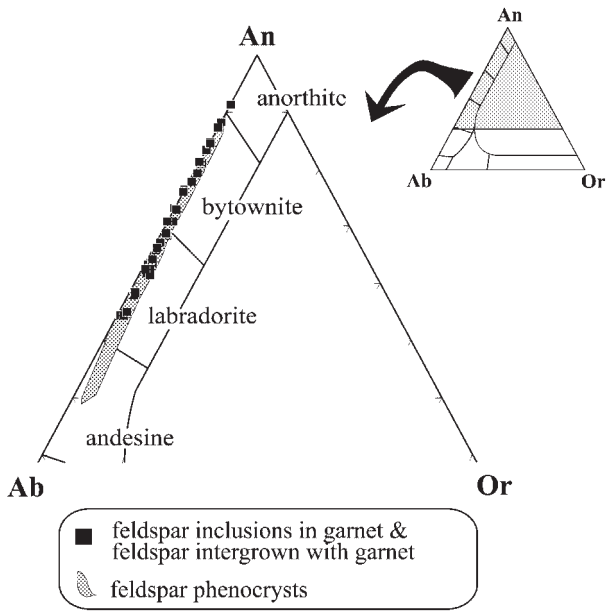

Fig. 7. Compositional variation of feldspars coexisting with garnets in the Ab–An–Or diagram. Plagioclases intergrown with garnet and occurring as inclusions in the garnets are An rich and overlap the compositional field of the cores of plagioclase phenocrysts.

whereas those in the more acidic rocks have sharp margins, euhedral or rounded shapes and lack reaction rims. The varying degree of resorption and the occurrence of reaction coronae may reflect differences in the speed of magma ascent. We infer that the rhyodacitic magma carrying the Type 1A garnets ascended and erupted rapidly. The rapid ascent prevented reaction and preserved the euhedral garnet shapes. The low amount of phenocrysts and the glassy groundmass of these rocks also support this idea. In contrast, the andesitic magmas could have had a slower ascent rate, so breakdown and resorption of early-formed Type 2 garnets took place at lower pressure.

The cores of composite garnets (Type 3) are in turn unambiguously xenocrysts, on the basis of their different chemical composition (low CaO and variable MnO contents) and their distinct inclusion assemblage (e.g. MnO-bearing biotite and orthopyroxene) or their enclosed metamorphic rock fragments (Fig. 2g). In the NPB, garnet occurs in different metamorphic rocks (amphibolite, gneiss, micaschist) within the crystalline basement, but these garnets have clearly different compositions compared with the cores of the composite garnets (Koroknai *et al.*, 1999). Almandines in the gneisses are pyrope rich (Pyr 17–19 mol %), whereas they have a significant grossular component (Gro 18–20 mol %) in the amphibolites. In addition, K/Ar and Ar/Ar ages as well as zircon fission-track data indicate rapid extensional unroofing during the Late Cretaceous (Koroknai *et al.*, 1999). Thus, these rocks were situated at shallow crustal levels at the time of the calc-alkaline volcanism (Middle Miocene). As the low-Ca Type 3 garnet cores are overgrown by primary garnet zones inferred to have crystallized at high pressure, these shallow crustal metamorphic rocks are unlikely to be a potential source for the xenocrystic garnet cores. Almandine garnets from the crustal xenolith in an andesite of the Visegrád Mts (Type 4 garnet) have a very different chemical composition (high MnO content) compared with the xenocrystic Type 3 garnet cores (Tables 2 and 3). Therefore, this metamorphic rock fragment also cannot represent the source rock of the low-Ca garnet cores. The crustal xenolith enclosed by the light-coloured core of a rounded garnet phenocryst in the Nógrád dacite (Fig. 2g), however, may provide some information about the source of the low-Ca garnets. This rock fragment consists of corundum, pleonaste and biotite and represents an Al-rich composition. Thus, this xenolith-bearing Ca-poor garnet may represent a restite formed by anatexis of a lower-crustal metapelite. The REE pattern of the light-coloured core of a Type 3 garnet has stronger negative Eu anomaly and higher Gd/Dy_N ratio than the primary garnet types (Fig. 4) and resembles that of garnets from granulite-grade metapelites (e.g. Bea *et al.*, 1997; Bea & Montero, 1999). The irregular contacts and incomplete resorption between the garnet xenocrysts and the garnet overgrowth indicate reactions between the incorporated garnet fragments and the ascending melt.

Primary igneous garnets have great petrogenetic significance, because their composition depends on the magma type and the pressure and temperature under which they crystallize (Green, 1977, 1992). High-pressure almandines from mantle-derived (M-type) or I-type magmas (Table 1) are characterized by relatively high CaO (>5 wt %) and low MnO (<2 wt %) contents (Fig. 11a). With decreasing pressure, MnO content increases (>3 wt %), whereas CaO remains relatively high (>4 wt %). In contrast, almandines from S-type magmas (Table 1) and from metapelites have low CaO content (<4 wt %) and variable MnO concentration (Fig. 11a). The compositions of primary almandines of the NPB (Fig. 11a) are consistent with crystallization dominantly from M-type or I-type magmas at high pressure, probably at the mantle–crust boundary zone. Chemical compositions of the amphiboles coexisting with garnets support the high-pressure origin. Most of them crystallized at higher pressures and temperatures than amphiboles in the garnet-free magmas (Fig. 6). On the basis of the CaO and MnO contents of the garnets and the composition of the coexisting amphiboles, Type 1B garnets could have formed at higher pressure than the Type 2 garnets. The mineral assemblage occurring with garnets (Ca-rich plagioclase, magnesiohastingsitic and tschermakitic amphibole) also indicates mantle-derived host

Table 9: Representative chemical composition of ilmenites and pleonaste occurring as inclusions in garnets or as microphenocrysts (for abbreviations see Table 6)

Locality:	Morgó hill (VM)	Bajdázó quarry (BM)		Castle hill, Nógrád (BM)			Királyrét (BM)	Šiatoroš (Karancs)		Breziny (CSVF)	
Sample:	ps4	b26		l-nv			krb1	sat1	sat2	S-B1	
Type:	incl in gt	mphcr	incl in gt	incl in gt	incl in am	incl in gt	incl in gt	incl in gt	incl in gt	incl in gt	mphcr
SiO_2	0·26	0·27	0·30	0·25	0·34	0·13	0·37	0·38	0·26	0·28	0·27
TiO_2	0·17	52·07	52·19	52·57	48·74	0·16	52·65	48·84	49·26	48·18	47·73
Al_2O_3	60·08	0·27	0·16	0·24	0·26	59·52	0·27	0·26	0·17		
FeO	33·43	46·08	45·30	44·95	43·96	33·06	46·25	47·08	47·79	47·37	49·16
MnO	0·09	0·37	0·33	0·25	0·31		0·40	0·91	0·71	0·73	0·70
MgO	6·80	0·85	1·30	1·22	3·27	6·43	1·31	1·41	1·01		0·95
CaO	0·11				0·42						
Total	100·94	99·91	99·58	99·48	97·30	99·30	101·25	98·88	99·20	96·56	98·81
Cations based on 3 (ilmenite) and 4 (pleonaste) oxygens											
Si	0·0070	0·0066	0·0074	0·0062	0·0085	0·0035	0·0090	0·0094	0·0064	0·0072	0·0067
Ti	0·0034	0·9807	0·9832	0·9915	0·9204	0·0032	0·9747	0·9221	0·9310	0·9442	0·9054
Al	1·9404	0·0078	0·0046	0·0070	0·0076	1·9553	0·0077	0·0076	0·0049		
Fe^{2+}	0·7286	0·9490	0·9359	0·9428	0·7898	0·7403	0·9282	0·8606	0·8854	0·9358	0·8620
Fe^{3+}	0·0374	0·0161	0·0131		0·1334	0·0302	0·0239	0·1280	0·1190	0·0965	0·1750
Mn	0·0019	0·0077	0·0069	0·0053	0·0065		0·0082	0·0192	0·0150	0·0160	0·0149
Mg	0·2776	0·0317	0·0484	0·0456	0·1223	0·2670	0·0480	0·0527	0·0378		0·0356
Ca	0·0031				0·0112						
Ilm (%)		99·17	99·32	100·00	92·74		98·76	93·30	93·85	95·12	90·99

Table 10: Representative chemical composition of the garnet-bearing volcanic rocks of the NPB; initial $^{87}Sr/^{86}Sr$ ratios are calculated using 15 Ma age for the formation of the volcanic rocks

	Visegrád Mts					
Locality:	Morgó hill	Szentlélek hill	Holdvilág creek	Holdvilág creek	Dömös	Csódi hill
Sample:	ps4	ps6	cs5	h1	l2	csh
Major elements (wt %)						
SiO_2	70·08	70·01	68·64	68·90	70·51	66·16
TiO_2	0·15	0·14	0·19	0·18	0·18	0·25
Al_2O_3	16·22	16·31	16·56	16·48	16·75	17·48
Fe_2O_3	2·95	3·13	3·67	3·36	4·11	4·13
MnO	0·04	0·05	0·07	0·06	0·04	0·10
MgO	0·26	0·28	0·36	0·38	0·40	0·65
CaO	2·92	2·79	3·23	3·36	2·23	4·24
Na_2O	3·66	3·48	3·09	3·60	2·88	3·53
K_2O	3·24	3·42	3·56	3·06	3·07	2·69
P_2O_5	0·11	0·10	0·14	0·14	0·14	0·18
Total	99·63	99·71	99·51	99·52	100·31	99·41
LOI	1·64	2·23	2·30	0·92	2·37	0·97
Trace elements (ppm)						
Ni	4	4	4	4	3	4
Cr	4	4	4	8	4	4
V	4	5	7	17	8	15
Sc	2·9	3·1	3·3	2·5	2·9	4·4
Rb	125	127	121	112	118	107
Ba	661	643	659	666	666	678
Pb	31·9	31·7	31·9	32·3	29·0	28·6
Sr	276	262	296	303	214	340
Zr	214	212	203	197	202	187
Nb	13	13	12	11	11	10
Y	10	16	14	11	14	17
Th	15·9	15·7	15·1	15·5	14·1	13·0
La	39·64	44·60	41·30	39·00	33·35	34·51
Ce	80·34	78·60	76·20	77·12	65·67	67·17
Nd	30·70	34·60	30·50	27·10	26·99	22·60
Sm	5·38			4·56	4·15	3·60
Eu	1·22			1·18	1·01	1·00
Gd	4·19			3·54		2·96
Dy	2·25			2·24		2·51
Ho	0·33			0·37		0·49
Er	0·52			0·64		1·20
Yb	0·48			0·67	0·77	1·53
Lu	0·07			0·10	0·11	0·26
Radiogenic isotope ratios						
$(^{87}Sr/^{86}Sr)_m$	0·71034	0·71036	0·71002	0·71001	0·70996	0·70939
$(^{87}Sr/^{86}Sr)_o$	0·71004	0·71004	0·70975	0·70977	0·70960	0·70918
$(^{143}Nd/^{144}Nd)_m$	0·51230			0·51231		0·51235

	Börzsöny			Karancs		CSVF
Locality:	Castle hill, Nógrád	Bajdázó quarry	Nagykő hill	Šiatoroš	Farkasnyak	Breziny
Sample:	I-nv	B26	B2L	sat2	kar1	S-B1
Major elements (wt %)						
SiO_2	64·46	63·28	61·96	61·62	58·16	60·84
TiO_2	0·56	0·56	0·71	0·56	0·67	0·71
Al_2O_3	18·56	18·76	18·28	17·65	18·55	17·38
Fe_2O_3	3·82	4·08	5·51	6·43	7·67	6·72
MnO	0·04	0·05	0·07	0·15	0·18	0·14
MgO	0·91	1·15	1·92	2·03	2·80	2·34
CaO	5·64	6·61	5·87	6·09	7·31	5·90
Na_2O	3·13	3·12	2·89	3·18	2·79	3·13
K_2O	2·52	2·49	2·49	2·03	1·66	2·11
P_2O_5	0·16	0·16	0·18	0·18	0·18	0·22
Total	99·80	100·26	99·88	99·92	99·97	99·49
LOI	2·48	3·52	1·19	0·99	3·41	0·38
Trace elements (ppm)						
Ni	6	7	8	5	5	4
Cr	10	11	17	14	17	7
V	44	43	61	80	129	94
Sc	6·9	6·5	9·7	14·6	20·6	12·5
Rb	113	114	117	77	66	83
Ba	534	525	505	311	293	448
Pb	24·3	24·4	22·8	12·7	10·3	13·7
Sr	379	387	359	358	343	367
Zr	141	139	142	112	110	151
Nb	10	10	10	8	6	17
Y	5	6	11	21	21	21
Th	10·9	11·0	9·0	8·1	6·1	9·4
La	31·00	30·60	24·31	21·11	16·90	30·73
Ce	58·70	59·20	52·25	44·30	34·90	60·32
Nd	27·00	27·70	23·70	18·50	15·90	22·70
Sm			4·84	3·67		4·15
Eu			1·41	1·05		1·23
Gd			3·88	3·61		3·96
Dy			2·32	3·36		3·46
Ho			0·40	0·66		0·68
Er			0·81	1·70		1·68
Yb			0·82	1·93		1·84
Lu			0·13	0·31		0·30
Radiogenic isotope ratios						
$(^{87}Sr/^{86}Sr)_m$	0·71015	0·71019	0·71011	0·70707	0·70629	0·70700
$(^{87}Sr/^{86}Sr)_o$	0·70995	0·71000	0·70991	0·70694	0·70617	0·70685
$(^{143}Nd/^{144}Nd)_m$			0·51234	0·51244		0·51246

m, measured; o, initial at 15 Ma.

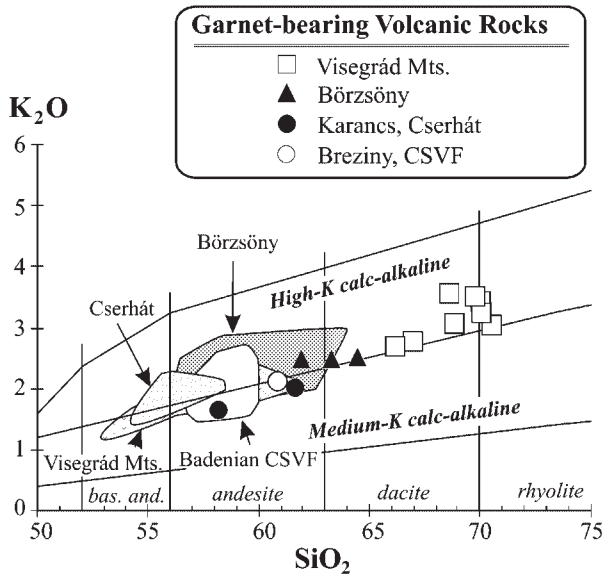

Fig. 8. SiO_2 vs K_2O classification diagram (Gill, 1981) for garnet-bearing volcanic rocks of the NPB compared with garnet-free volcanic series from the same volcanic fields (Downes *et al.*, 1995; Sz. Harangi & H. Downes, unpublished data, 1998). Within the Central Slovakian Volcanic Field (CSVF), only the Badenian (Middle Miocene) volcanic products are shown for comparison.

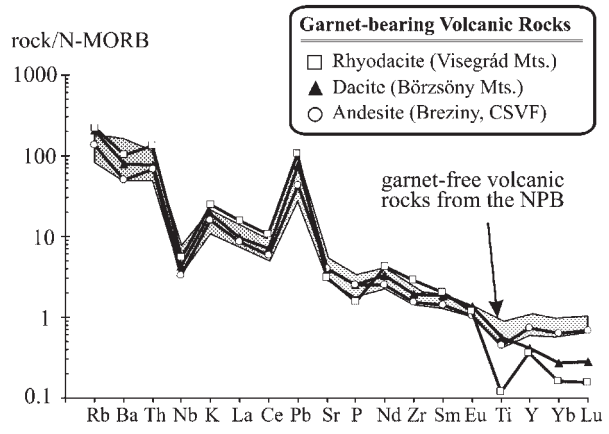

Fig. 9. Representative N-MORB (Pearce & Parkinson, 1993) normalized trace element patterns for garnet-bearing volcanic rocks of the NPB compared with the range of garnet-free volcanic products from the same areas (Sz. Harangi & H. Downes, unpublished data, 1998).

magmas. The slightly peraluminous character of the rhyodacites may suggest an S-type origin; however, the relatively high CaO and low MnO contents of the Type 1A garnets (Table 2, Fig. 11a) are inconsistent with an S-type affinity. We suggest that the peraluminous character of the rhyodacites could be the result of contamination by a large amount of lower-crustal metapelitic material. Cores of composite (Type 3) garnets fall in the fields of almandines from S-type magmas and from metapelites (Fig. 11b). Most of them have low MnO

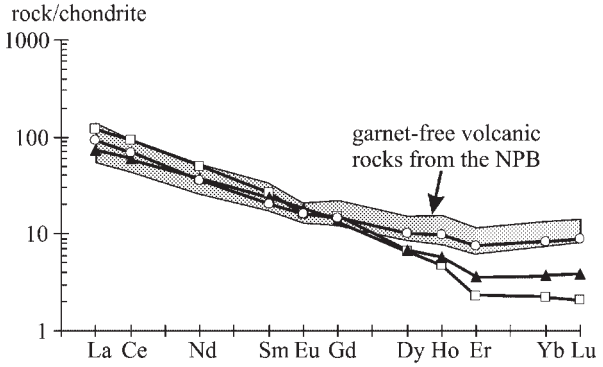

Fig. 10. Representative chondrite (Nakamura, 1974) normalized REE patterns for garnet-bearing volcanic rocks of the NPB compared with the range of garnet-free volcanic products from the same areas (Sz. Harangi & H. Downes, unpublished data, 1998). Symbols as in Fig. 9.

contents (<3 wt %), in contrast to the Type 4 almandines from the crustal xenolith (Table 2; Fig. 11b). These garnet fragments may be derived from a heterogeneous lower crust. Type 3 garnet overgrowths have compositions similar to the Type 1B and Type 2 garnets inferred to have a high-pressure origin. This suggests that the xenocrystic Type 3 garnet fragments were incorporated into the host magmas at lower-crustal depths.

Pressure and temperature constraints

Chemical compositions of the NPB garnets and the coexisting minerals suggest that they formed at high pressures and temperatures. Intergrowths of these minerals imply that they are a magmatic equilibrium assemblage and therefore they can be used to quantify the temperature and pressure conditions under which the garnets crystallized. Phase equilibrium diagrams (e.g. Green, 1982, 1992; Huang & Wyllie, 1986; Conrad *et al.*, 1988) may also help to constrain the pressure–temperature conditions of crystallization. The phenocryst assemblage in the NPB volcanic rocks consists of plagioclase, amphibole and/or biotite and garnet. According to experimental results (e.g. Clemens & Wall, 1981; Green, 1982, 1992; Huang & Wyllie, 1986; Conrad *et al.*, 1988), the absence of quartz and presence of plagioclase, amphibole and/or biotite in a dacitic liquid suggest magma H_2O content close to 5 wt % and crystallization temperature above 800°C. A higher water content in the magma strongly suppresses plagioclase crystallization, whereas a lower H_2O content expands the quartz field and reduces the amphibole field. A mineral assemblage of garnet + plagioclase + amphibole is stable at 8–13 kbar and 820–920°C in a dacitic magma with 5% H_2O (Green, 1992).

Among the geothermometers and geobarometers that use the mineral assemblage characteristic of the NPB

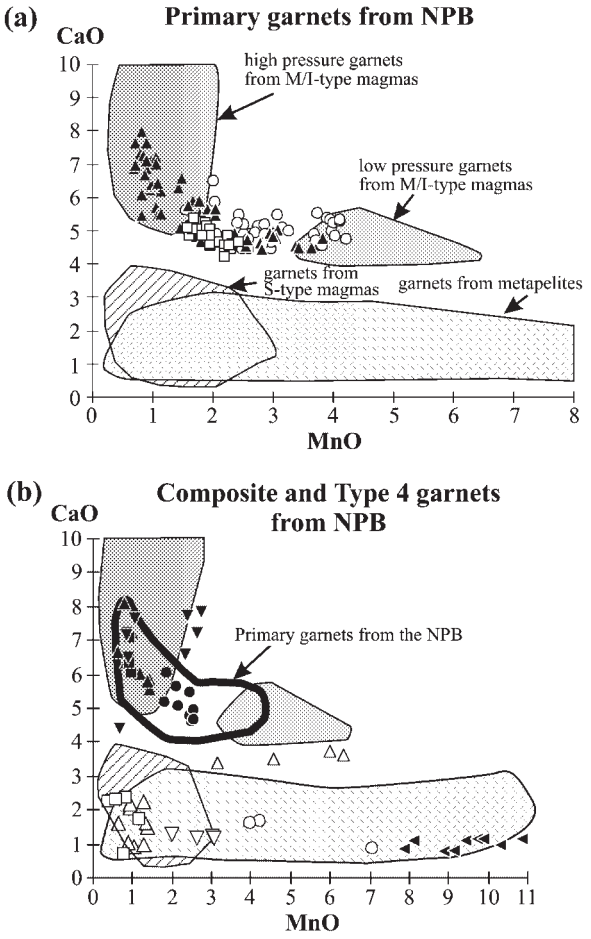

Fig. 11. CaO vs MnO plot for (a) primary (Type 1A, 1B and 2) garnets and (b) composite (Type 3) and Type 4 garnets of the NPB. For comparison, fields are shown for almandines from selected M/I-type magmas (Northland, New Zealand, Day *et al.*, 1992; Mt Somers, New Zealand, Barley, 1987; Central Caucasus, Tsvetkov & Borisovskiy, 1980; Yamanogawa, Japan, Kano & Yashima, 1976; Martinique, Lesser Antilles, Maury *et al.*, 1985), S-type magmas (Mt Misery, New Zealand, Barley, 1987; Victoria, Australia, Green & Ringwood, 1968; Clemens & Wall, 1984; Kamitazawa, Japan, Kano & Yashima, 1976; Borrowdale, Lake District, Fitton, 1972) and from metapelites (French Massif Central, Bertaux, 1982; Western Alps, Bea *et al.*, 1997; Rangeley formation, Kohn *et al.*, 1997). (Note the clear separation of almandines from M/I-type and S-type magmas based on the CaO content of the garnets.) Symbols as in Fig. 3.

garnet-bearing volcanic rocks, only two appear to be applicable considering the conditions of calibration. The amphibole–plagioclase (Blundy & Holland, 1990; Holland & Blundy, 1994) and the biotite–garnet (e.g. Ferry & Spear, 1978; Holdaway *et al.*, 1997) thermometers can give the temperature range when garnet crystallized together with these minerals.

Amphibole compositions (high Al^{iv} and Na + K; Fig. 6) in the garnet-bearing volcanic rocks suggest that they crystallized at a relatively high temperature range. Correlation between Al^{iv} and $(Na + K)^{[A]}$ and between Si and $Al^{iv} + (Na + K)^{[A]}$ in amphiboles implies edenite substitution. In addition, Ti-tschermakite substitution could be also important, as indicated by the correlation between Al^{iv} and Ti. Both substitutions are temperature dependent, such that higher temperature can greatly increase Al^{iv} in hornblende (e.g. Helz, 1973; Anderson & Smith, 1995). The Holland & Blundy (1994) amphibole–plagioclase thermometer using a plagioclase compositional range of $X_{ab} = 0{\cdot}2–0{\cdot}4$ and pressure of 7–8 kbar gave an equilibrium temperature of 840–940°C.

Coexisting garnet and biotite may be used to estimate crystallization temperature by applying the Fe–Mg exchange geothermometer originally calibrated by Ferry & Spear (1978). Later calibrations took into account non-ideal mixing behaviour in these minerals and incorporated a correction for Mn and Ca content in garnet and Al^{vi} and Ti in biotite (e.g. Indares & Martignole, 1985; Kleeman & Reinhardt, 1994; Holdaway *et al.*, 1997). Holdaway *et al.* (1997) emphasized also the role of Fe^{3+} in the calibration compositions. This latter geothermometer yields temperatures from 700°C (Type 1B garnets) to 780°C (Type 1A garnets) for the coexisting garnet and biotite pairs of the NPB volcanic rocks. In contrast, the Ferry & Spear (1978) geothermometer gives significantly higher temperatures, ranging from 730°C (Type 1B garnets) to 880°C (Type 1A garnets). The relatively high temperature for the Type 1A garnets is consistent with the results obtained by Clemens & Wall (1984) for the Violet Town peraluminous rhyolites (~830°C) and Barley (1987) for the Mt Somers dacites (~880°C) using also the Ferry & Spear (1978) calibration. It indicates an early magmatic equilibrium assemblage, where biotite and garnet are the main near-liquidus ferromagnesian phases (Clemens & Wall, 1981). In contrast, the low temperature (~700°C) for the Type 1B garnet and biotite pairs seems to be unreasonably low considering the phase equilibria conditions.

In conclusion, phase equilibria results on dacitic melt and the applied geothermometers indicate that garnets from the NPB volcanic rocks could have formed in the temperature range of 800–940°C. The majority of NPB primary garnets have relatively high grossular content (>10 mol %) consistent with a high-pressure (>7 kbar) origin (Green, 1977, 1992). The absence of quartz and the presence of plagioclase with garnet, amphibole and/or biotite suggest a magma H_2O content close to 5 wt %. This volatile content might have enhanced the rapid ascent of the magmas from lower-crustal depths.

Genesis of the garnet-bearing volcanic rocks

Almandine-bearing magmas can be classified as S-type and I- or M-type melts following the scheme for silicic

igneous rocks proposed by Chappell & White (1974) and adopted by Green (1992) for garnet-bearing volcanic rocks. Almandine phenocrysts are more common in S-type (peraluminous) magmas (Table 1), i.e. in melts generated by anatexis of metapelitic formations. Such almandines are usually associated with plagioclase, biotite, quartz, K-feldspar and cordierite. Garnet-bearing metapelitic xenoliths are also common in these rocks (e.g. Zeck, 1970; Wood, 1974; Munksgaard, 1984; Barker, 1987). On the other hand, almandine can also occur in I-type magmas, i.e. melts derived by partial melting of igneous rocks in the crust or M-type melts from the upper mantle. These volcanic rocks are diopside-normative and have A/CNK ratios <1, i.e. metaluminous. In these rocks, almandine has a considerable Ca content (Gro >10 mol %) and coexists with plagioclase, amphibole, biotite, orthopyroxene and rarely with clinopyroxene. Table 1 demonstrates that garnet-bearing I-type and especially M-type volcanic rocks are not as rare as once thought (Green, 1992).

Primary almandine in the NPB volcanic rocks crystallized at 7–12 kbar, i.e. ~25–35 km depth. As the present crustal thickness beneath this area is 28–32 km, this depth corresponds to the crust–mantle boundary, as assumed previously by Embey-Isztin *et al.* (1985) from the experimental results of Green (1982). This also suggests that the primary host magmas were mantle derived. Indeed, the garnet-bearing andesites and some dacites have diopside-normative compositions. On the other hand, the more silicic rocks containing Type 1A garnets are slightly peraluminous and therefore may have been formed by anatexis of metapelites or by extensive contamination of mantle-derived magma. However, garnets in the rhyodacites do not support this origin because their compositions do not resemble almandines in S-type volcanic rocks (Fig. 11a) and they do not coexist with typical 'S-type' minerals. Therefore, we conclude that the slightly peraluminous silicic magmas could have evolved from metaluminous liquids either by high-pressure fractionation of clinopyroxene and amphibole (Ellis & Thompson, 1986; Conrad *et al.*, 1988; Green, 1992) or by significant lower-crustal contamination. The isotopic compositions of the host rocks and the narrow curvilinear trend in the Sr–Nd isotope diagram (Fig. 12c) indicate involvement of a crustal component. Source contamination alone is unlikely to be responsible for the increase of radiogenic Sr in the host magmas and the $\delta^{18}O$ values of garnets (Fig. 12a and b). Assimilation of upper-crustal rocks can be also excluded, because it is not consistent with either the depth (~30 km) of origin of the garnets or the Sr–Nd–O isotopic trends. Assimilation of the fusible part of the lower crust could, however, explain these trends (Fig. 12a and b). The low-Ca xenocrystic cores in the Type 3 garnets and their inclusions provide evidence for the presence of metapelitic material in the lower crust beneath the NPB. Embey-Isztin *et al.* (2000) recently described metasedimentary lower-crustal xenoliths from the Pannonian Basin with a high proportion of Al-rich mineral phases. The linear trend in the $\delta^{18}O^{minerals}$ vs $(^{87}Sr/^{86}Sr)_{host\ rock}$ diagram (Fig. 12a and b) can be explained by two-component mixing between a mantle-derived magma and crustal material with a relatively low $\delta^{18}O$ value, high $^{87}Sr/^{86}Sr$ ratio and similar Sr content to that of the magma. The $^{87}Sr/^{86}Sr$ and $^{143}Nd/^{144}Nd$ isotope ratios of metasedimentary granulite xenoliths from the Pannonian Basin (Embey-Isztin *et al.*, 2000) and the French Massif Central (Downes *et al.*, 1990; Kempton & Harmon, 1992) are consistent with such a crustal end-member. The high $\delta^{18}O$ value (10·5‰) of the Type 3 garnet core from Verőce (Börzsöny Mts) indicates that it could be a fragment of this metapelitic lower crust. Mixing calculations suggest 20–25% lower-crustal component in the garnet-bearing andesites and 40–50% lower-crustal component in the rhyodacites. Such a large amount of assimilation requires a high heat flow beneath the NPB during the Miocene. This could be a result of upwelling of hot asthenosphere as a result of the thinning of the lithosphere and the intrusion of mantle-derived magmas.

Almandine garnets occur only in evolved magmas in the NPB. The strong correlation between most LILE and high field strength elements (HFSE) (e.g. Rb, Ba, La, Th, Zr, Nb) and SiO_2 content in the garnet-bearing rocks implies that these elements behaved incompatibly throughout the magma evolution. In contrast, Sr and the HREE decrease in the more silicic rocks, consistent with fractionation of plagioclase, garnet and amphibole. The lack of a strong negative Eu anomaly in the REE pattern of garnet-bearing andesites and dacites (Fig. 10) indicates that plagioclase did not play an important role in the early crystallization stage, but formed simultaneously with garnet. Indeed, the HREE-depleted rhyodacites show a negative Eu anomaly ($Eu/Eu^* = 0{\cdot}76–0{\cdot}87$; Fig. 10). The considerable depletion of HREE could be a result of garnet fractionation. Zircon fractionation could also decrease the HREE concentration in evolved liquids, but the incompatible behaviour of Zr in the NPB rocks excludes this process. However, this simple scenario does not explain the anomalously low HREE content of the dacites from the Börzsöny Mts (Fig. 10). These rocks contain <11 ppm Y, whereas the rhyodacites have 10–16 ppm Y, but similar radiogenic isotopic compositions (Table 10). Fractional crystallization could not result in this HREE variation, therefore residual garnet is inferred to have been present during partial melting.

Crystallization of garnet, absence of quartz, and presence of amphibole and/or biotite require some water in the host magma, but the additional presence of plagioclase suggests that the water content cannot be higher than ~5 wt % (e.g. Green, 1982, 1992; Huang & Wyllie,

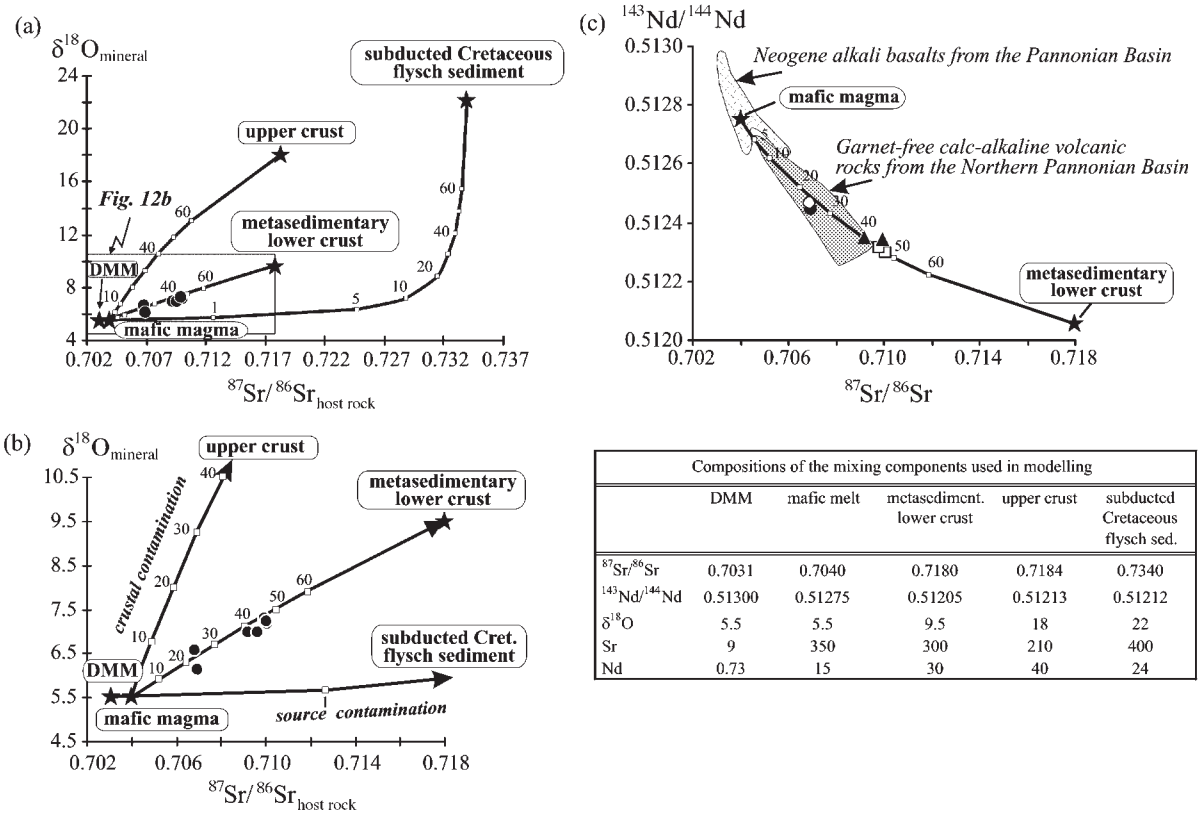

Compositions of the mixing components used in modelling

	DMM	mafic melt	metasediment. lower crust	upper crust	subducted Cretaceous flysch sed.
$^{87}Sr/^{86}Sr$	0.7031	0.7040	0.7180	0.7184	0.7340
$^{143}Nd/^{144}Nd$	0.51300	0.51275	0.51205	0.51213	0.51212
$\delta^{18}O$	5.5	5.5	9.5	18	22
Sr	9	350	300	210	400
Nd	0.73	15	30	40	24

Fig. 12. Petrogenetic modelling for the origin of the garnet-bearing magmas from the NPB based on the oxygen isotope composition of garnets and $^{87}Sr/^{86}Sr$ ratios of the host rocks (a) and (b); and the Sr–Nd isotope composition of garnet-bearing volcanic rocks (c). The garnet and the host rock isotopic trends can be modelled by two-component mixing between mantle-derived mafic magma and metasedimentary lower crust. DMM, Depleted MORB Mantle; data for sedimentary lower crust are based on Downes *et al.* (1990), Kempton & Harmon (1992) and Embey-Isztin *et al.* (2000); data for the upper crust and the subducted Cretaceous flysch sediment are based on Mason *et al.* (1996). Additional data for comparison: Neogene alkali basalts: Embey-Isztin *et al.* (1993); Dobosi *et al.* (1995); Harangi *et al.* (1995); garnet-free calc-alkaline volcanic rocks: Sz. Harangi & H. Downes, unpublished data (1998). Symbols as in Fig. 8.

1986). It indicates also a hydrous mantle source unless a significant amount of H_2O-rich crustal material was incorporated into the magma. A potential hydrous mantle source could be metasomatized lithospheric mantle. The presence of amphibole and phlogopite in ultramafic xenoliths in alkaline basalts of the NPB (Szabó & Taylor, 1994) and silicate melt inclusions and melt pockets interpreted as infiltration of calc-alkaline melts (Szabó *et al.*, 1996) suggest extensive metasomatism of the lithospheric mantle beneath the NPB. Much of this metasomatism could be related to an earlier subduction event.

Geodynamic implications of eruption of garnet-bearing magmas

Garnet-bearing volcanic rocks are volumetrically rare worldwide. As Mn-poor almandine is not stable at shallow depths (Green, 1977), rapid ascent of a garnet-bearing magma is necessary to preserve this mineral. This requires the presence of deep-seated faults or tectonically weak zones and a tensional stress field. In addition, crystallization of almandine is favoured from silicate liquid with a high water content, so a hydrous mantle source is another essential requirement. These circumstances could be attained in areas that undergo lithospheric stretching following (or concurrent with) subduction. Most garnet-bearing volcanic rocks worldwide appear to be related to such regions. In the Neogene volcanic field of SE Spain (e.g. Doblas & Oyarzun, 1989; Benito *et al.*, 1999; Zeck, 1999), volcanic activity took place during syn- and post-extensional phases, which followed subduction and continental collision. In the Pyrenees, a Permo-Carboniferous garnet-bearing volcanic series formed during the Hercynian orogeny, when extension followed collision (Gilbert & Rogers, 1989). Barley (1987) proposed that the Cretaceous Canterbury volcanic rocks in New Zealand were formed when the tectonic regime changed from compression to extension. The Miocene volcanism of the Northland region (New Zealand) occurred in a post-obduction–subduction tectonic setting,

when partial melting took place in a hydrous mantle source (Smith *et al.*, 1989; Day *et al.*, 1992).

In the NPB, the Middle Miocene (13–18 Ma) geodynamic circumstances could also have favoured eruption of garnet-bearing magmas. In the West Carpathians, active subduction was already terminated by this time (e.g. Meulenkamp *et al.*, 1996), but it was the main period of formation of the Pannonian Basin by large-scale lithospheric extension (e.g. Csontos *et al.*, 1992; Tari & Horváth, 1995). The present-day thin crust and especially the thin lithosphere beneath the NPB (Horváth, 1993) imply that this region underwent lithospheric extension. Nemčok & Lexa (1990) suggested syn-volcanic extensional tectonic activity and a Basin and Range-type structure for the Central Slovakian Volcanic Field. The garnet-bearing volcanic rocks are remarkably situated along major tectonic lines (Fig. 1b). Therefore, independent lines of evidence support the contention that the Miocene calc-alkaline volcanism in the Northern Pannonian Basin that started with the eruption of garnet-bearing magmas at $\sim$16 Ma was related to extension following subduction. The occurrence of garnet-bearing volcanic rocks may imply a change in the tectonic regime in this area and suggest a tensional stress field in Mid-Miocene time.

ACKNOWLEDGEMENTS

Radiogenic and stable isotope and X-ray fluorescence facilities at Royal Holloway are University of London Intercollegiate Research Services. We thank Gerry Ingram and Giz Marriner for their assistance. Andy Beard is acknowledged for helpful assistance during the microprobe work at Birkbeck College. Sz.H.'s research was supported by a NATO post-doctoral research fellowship from the Royal Society. Fieldwork was financially supported by the Hungarian Research Fund (OTKA T025833) and the University of London Central Research Fund. Thanks are due to J. P. Davidson, T. H. Green and J. G. Fitton for their helpful and constructive reviews.

REFERENCES

Abdel-Rahman, A. M. (1994). Nature of biotites from alkaline, calc-alkaline, and peraluminous magmas. *Journal of Petrology* **35**, 525–541.

Anderson, J. L. & Smith, D. R. (1995). The effects of temperature and fO_2 on the Al-in-hornblende barometer. *American Mineralogist* **80**, 549–559.

Baker, J. A., Menzies, M. A., Thirlwall, M. F. & Macpherson, C. G. (1997). Petrogenesis of Quaternary intraplate volcanism, Sana'a, Yemen: implications for plume–lithosphere interaction and polybaric melt hybridization. *Journal of Petrology* **38**, 1359–1390.

Balla, Z. (1981). Neogene volcanism of the Carpatho-Pannonian region. *Earth Evolution Science* **3–4**, 240–248.

Barker, D. S. (1987). Rhyolites contaminated with metapelite and gabbro, Lipari, Aeolian Islands, Italy: products of lower crustal fusion or of assimilation plus fractional crystallisation? *Contributions to Mineralogy and Petrology* **97**, 460–472.

Barley, M. E. (1987). Origin and evolution of Mid-Cretaceous garnet-bearing, intermediate and silicic volcanics from Canterbury, New Zealand. *Journal of Volcanology and Geothermal Research* **32**, 247–267.

Bea, F. & Montero, P. (1999). Behavior of accessory phases and redistribution of Zr, REE, Y, Th, and U during metamorphism and partial melting of metapelites in the lower crust: an example from the Kinzigite Formation of Ivrea–Verbano, NW Italy. *Geochimica et Cosmochimica Acta* **63**, 1133–1153.

Bea, F., Montero, P., Garuti, G. & Zacharini, F. (1997). Pressure-dependence of rare earth element distribution in amphibolite- and granulite-grade garnets. A LA-ICP-MS study. *Geostandards Newsletter* **21**, 253–270.

Benito, R., López-Ruiz, J., Cebriá, J. M., Hertogen, J., Doblas, M., Oyarzun, R. & Demaiffe, D. (1999). Sr and O isotope constraints on source and crustal contamination in the high-K calc-alkaline and shoshonitic Neogene volcanic rocks of SE Spain. *Lithos* **46**, 773–802.

Bertaux, J. (1982). Origine métamorphique des grenats des volcanites acides d'âge viséen supérieur dans le nord-est du Massif Central français. *Bulletin de Minéralogie* **105**, 212–222.

Birch, W. D. & Gleadow, A. J. W. (1974). The genesis of garnet and cordierite in acid volcanic rocks: evidence from the Cerberean Cauldron, Central Victoria, Australia. *Contributions to Mineralogy and Petrology* **45**, 1–13.

Bleahu, M., Boccaletti, M., Manetti, P. & Peltz, S. (1973). The Carpathian Arc: a continental arc displaying the features of an 'island arc'. *Journal of Geophysical Research* **78**, 5025–5032.

Blundy, J. D. & Holland, T. J. B. (1990). Calcic amphibole equilibria and a new amphibole–plagioclase geothermometer. *Contributions to Mineralogy and Petrology* **104**, 208–224.

Boccaletti, M., Manetti, P., Peccerillo, A. & Peltz, S. (1973). Young volcanism in the Calimani–Harghita Mountains (East Carpathians): evidence of a palaeoseismic zone. *Tectonophysics* **19**, 299–313.

Brousse, R., Bizouard, H. & Salát, J. (1972). Grenats des andésites et des rhyolites de Slovaquie, origine des grenats dans les séries andésitiques. *Contributions to Mineralogy and Petrology* **35**, 201–213.

Chappell, B. W. & White, A. J. R. (1974). Two contrasting granite types. *Pacific Geology* **8**, 173–174.

Clemens, J. D. & Wall, V. J. (1981). Crystallisation and origin of some peraluminous (S-type) granitic magmas. *Canadian Mineralogist* **19**, 111–132.

Clemens, J. D. & Wall, V. J. (1984). Origin and evolution of a peraluminous silicic ignimbrite suite: the Violet Town Volcanics. *Contributions to Mineralogy and Petrology* **88**, 354–371.

Conrad, W. K., Nicholls, I. A. & Wall, V. J. (1988). Water-saturated and undersaturated melting of metaluminous and peraluminous crustal compositions at 10 kb: evidence for the origin of silicic magmas in the Taupo Volcanic Zone, New Zealand and other occurrences. *Journal of Petrology* **29**, 765–803.

Csontos, L., Nagymarosy, A., Horváth, F. & Kovác, M. (1992). Tertiary evolution of the Intra-Carpathian area: a model. In: Ziegler, P. A. (ed.) *Geodynamics of Rifting, Vol. I. Case Studies on Rifts: Europe and Asia. Special issue, Tectonophysics* **208**, 221–241.

Davidson, J. P. & Harmon, R. S. (1989). Oxygen isotope constraints on the petrogenesis of volcanic arc magmas from Martinique, Lesser Antilles. *Earth and Planetary Science Letters* **95**, 255–270.

Day, R. A., Green, T. H. & Smith, I. E. M. (1992). The origin and significance of garnet phenocrysts and garnet-bearing xenoliths in Miocene calc-alkaline volcanics from Northland, New Zealand. *Journal of Petrology* **33**, 125–161.

Doblas, M. & Oyarzun, R. (1989). Neogene extensional collapse in the western Mediterranean (Betic–Rif orogenic belt): implication for the genesis of the Gibraltar Arc and magmatic activity. *Geology* **17**, 430–433.

Dobosi, G., Fodor, R. V. & Goldberg, S. A. (1995). Late-Cenozoic alkali basalt magmatism in Northern Hungary and Slovakia: petrology, source compositions and relationship to tectonics. In: Downes, H. & Vaselli, O. (eds) *Neogene and Related Magmatism in the Carpatho-Pannonian Region. Special issue, Acta Vulcanologica*, **7**, 199–207.

Dobosi, G., Downes, H., Mattey, D. & Embey-Isztin, A. (1998). Oxygen isotope ratios of phenocrysts from alkali basalts of the Pannonian basin: evidence for an O-isotopically homogeneous upper mantle beneath a subduction-influenced area. *Lithos* **42**, 213–223.

Downes, H., Dupuy, C. & Leyreloup, A. F. (1990). Crustal evolution of the Hercynian belt of Western Europe: evidence from lower-crustal granulite xenoliths (French Massif Central). *Chemical Geology* **83**, 209–231.

Downes, H., Pantó, Gy., Póka, T., Mattey, D. P. & Greenwood, P. B. (1995). Calc-alkaline volcanics of the Inner Carpathian arc, Northern Hungary: new geochemical and oxygen isotopic results. In: Downes, H. & Vaselli, O. (eds) *Neogene and Related Magmatism in the Carpatho-Pannonian Region. Special issue, Acta Vulcanologica* **7**, 29–41.

Ellis, D. J. & Thompson, A. B. (1986). Subsolidus and partial melting reactions in the quartz-excess CaO–MgO–Al_2O_3–SiO_2–H_2O system under water-excess and water-deficient conditions to 10 kbar: some implications for the origin of peraluminous melts from mafic rocks. *Journal of Petrology* **27**, 91–121.

Embey-Isztin, A., Noske-Fazekas, G., Kurat, G. & Brandstätter, F. (1985). Genesis of garnets in some magmatic rocks from Hungary. *Tschermaks Mineralogische und Petrographische Mitteilungen* **34**, 49–66.

Embey-Isztin, A., Downes, H., James, D. E., Upton, B. G. J., Dobosi, G., Ingram, G. A., Harmon, R. S. & Scharbert, H. G. (1993). The petrogenesis of Pliocene alkaline volcanic rocks from the Pannonian Basin, Eastern Central Europe. *Journal of Petrology* **34**, 317–343.

Embey-Isztin, A., Downes, H., Dobosi, G. & Kempton, P. (2000). Geochemistry of lower crustal granulite xenoliths from Mindszentkálla and Sabarhegy, Pannonian Basin, Hungary. *Journal of Conference Abstracts* **5**, 383.

Ferry, J. M. & Spear, F. S. (1978). Experimental calibration of the partitioning of Fe and Mg between biotite and garnet. *Contributions to Mineralogy and Petrology* **66**, 113–117.

Fitton, J. G. (1972). The genetic significance of almandine–pyrope phenocrysts in the calc-alkaline Borrowdale Volcanic Group, Northern England. *Contributions to Mineralogy and Petrology* **36**, 231–248.

Gilbert, J. S. & Rogers, N. W. (1989). The significance of garnet in the Permo-Carboniferous volcanic rocks of the Pyrenees. *Journal of the Geological Society, London* **146**, 477–490.

Gill, J. B. (1981). *Orogenic Andesites and Plate Tectonics*. Berlin: Springer, pp. 1–390.

Green, T. H. (1976). Experimental generation of cordierite- or garnet-bearing granitic liquids from a pelitic composition. *Geology* **4**, 85–88.

Green, T. H. (1977). Garnet in silicic liquids and its possible use as a *P–T* indicator. *Contributions to Mineralogy and Petrology* **65**, 59–67.

Green, T. H. (1982). Anatexis of mafic crust and high pressure crystallisation of andesite. In: Thorpe, R. S. (ed.) *Andesites: Orogenic Andesites and Related Rocks*. Chichester: John Wiley, pp. 465–487.

Green, T. H. (1992). Experimental phase equilibrium studies of garnet-bearing I-type volcanics and high-level intrusives from Northland, New Zealand. *Transactions of the Royal Society of Edinburgh: Earth Sciences* **83**, 429–438.

Green, T. H. & Ringwood, A. E. (1968). Origin of the garnet phenocrysts in calc-alkaline rocks. *Contributions to Mineralogy and Petrology* **18**, 163–174.

Green, T. H. & Ringwood, A. E. (1972). Crystallization of garnet-bearing rhyodacite under high-pressure hydrous conditions. *Journal of the Geological Society of Australia* **19**, 203–212.

Günther, D., Frischknecht, R., Heinrich, C. A. & Kahlert, H.-J. (1997). Capabilities of an argon fluoride 193 nm excimer laser for laser ablation inductively coupled plasma mass spectrometry microanalysis of geological materials. *Journal of Analytical Atomic Spectrometry* **12**, 939–944.

Hamer, R. D. & Moyes, A. B. (1982). Composition and origin of garnet from the Antarctic Peninsula Volcanic Group of Trinity Peninsula. *Journal of the Geological Society, London* **139**, 713–720.

Harangi, S. (1999). Geochemistry and petrogenesis of the volcanic rocks of Csódi hill, Northern Hungary. *Topographia Mineralogica Hungariae, Miskolc* **6**, 59–85 (in Hungarian with English abstract).

Harangi, S. & Downes, H. (2000). Contrasting origins of Neogene calc-alkaline volcanic suites in the Carpathian–Pannonian region, Eastern–Central Europe. *Journal of Conference Abstracts* **5**, 484.

Harangi, S., Vaselli, O., Tonarini, S., Szabó, Cs., Harangi, R. & Coradossi, N. (1995). Petrogenesis of Neogene extension-related alkaline volcanic rocks of the Little Hungarian Plain Volcanic Field (Western Hungary). In: Downes, H. & Vaselli, O. (eds) *Neogene and Related Magmatism in the Carpatho-Pannonian Region. Special issue, Acta Vulcanologica* **7**, 173–187.

Harangi, S., Downes, H., Kósa, L. & Szabó, C. (1999). Genesis and geodynamic implications of garnets and garnet-bearing Miocene calc-alkaline volcanic rocks in the Northern Pannonian Basin, Central–Eastern Europe. *International Union of Geodesy and Geophysics 22nd General Assembly, University of Birmingham, School of Earth Sciences, Edgbaston, Birmingham, Abstract Volume* **B**, 73.

Helz, R. T. (1973). Phase relations of basalts in their melting range at P_{H_2O} = 5 kbar as function of oxygen fugacity. Part I. Mafic phases. *Journal of Petrology* **14**, 249–302.

Hensen, B. J. & Green, D. H. (1973). Experimental study of the stability of cordierite and garnet in pelitic compositions at high pressures and temperatures. *Contributions to Mineralogy and Petrology* **38**, 151–166.

Holdaway, M. J., Mukhopadhyay, B., Dyar, M. D., Guidotti, C. V. & Dutrow, B. L. (1997). Garnet–biotite geothermometry revised: new Margules parameters and a natural specimen data set from Maine. *American Mineralogist* **82**, 582–595.

Holland, T. & Blundy, J. (1994). Non-ideal interactions in calcic amphiboles and their bearing on amphibole–plagioclase thermometry. *Contributions to Mineralogy and Petrology* **116**, 433–447.

Horváth, F. (1993). Towards a mechanical model for the formation of the Pannonian Basin. In: Cloetingh, S., Sassi, W. & Horváth, F. (eds) *The Origin of Sedimentary Basins: Inferences from Quantitative Modelling and Basin Analysis. Tectonophysics* **226**, 333–357.

Huang, W. L. & Wyllie, P. J. (1986). Phase relationships of gabbro–tonalite–granite–water at 15 kbar with applications to differentiation and anatexis. *American Mineralogist* **71**, 301–316.

Indares, A. & Martignole, J. (1985). Biotite–garnet geothermometry in the granulite facies: the influence of Ti and Al in biotite. *American Mineralogist* **70**, 272–278.

Irving, A. J. & Frey, F. A. (1978). Distribution of trace elements between garnet megacrysts and host volcanic liquids of kimberlitic to rhyolitic composition. *Geochimica et Cosmochimica Acta* **42**, 771–787.

Kaličiak, M. I. & Žec, B. (1995). Review of Neogene volcanism of Eastern Slovakia. In: Downes, H. & Vaselli, O. (eds) *Neogene and Related Magmatism in the Carpatho-Pannonian Region. Acta Vulcanologica* **7**, 87–95.

Kano, H. & Yashima, R. (1976). Almandine-garnets of acid magmatic origin from Yamanogawa, Fukushima Prefecture and Kamitazawa, Yamagata Prefecture. *Journal of the Japan Association: Mineralogy, Petrology and Economic Geology* **71**, 106–119.

Kempton, P. D. & Harmon, R. S. (1992). Oxygen isotope evidence for large-scale hybridisation of the lower crust during magmatic underplating. *Geochimica et Cosmochimica Acta* **56**, 971–986.

Kleeman, U. & Reinhardt, J. (1994). Garnet–biotite thermometry revisited: the effect of Al^{vi} and Ti in biotite. *European Journal of Mineralogy* **6**, 925–941.

Kohn, M. J., Spear, F. S. & Valley, J. W. (1997). Dehydration-melting and fluid recycling during metamorphism: Rangeley formation, New Hampshire, USA. *Journal of Petrology* **38**, 1255–1277.

Konečný, V., Lexa, J. & Hojstricová, V. (1995). The Central Slovakia Neogene volcanic field: a review. In: Downes, H. & Vaselli, O. (eds) *Neogene and Related Magmatism in the Carpatho-Pannonian Region. Special issue, Acta Vulcanologica* **7**, 63–78.

Koroknai, B., Horváth, P., Balogh, K. & Dunkl, I. (1999). Alpine metamorphic evolution and cooling history of the Veporic crystalline basement in Northern Hungary: new petrological and geochronological constraints. *Tübinger Geowissenschaftliche Arbeiten* **A52**, 123–124.

Kósa, L. (1998). Gránátok genetikai jelentősége a Visegrádi-hegységben és a szomszédos vulkáni területeken. (Genetic significance of garnets from the Visegrád Mts. and the adjacent volcanic areas.) M.Sc. thesis, ELTE Közettani-Geokémiai Tanszék, Budapest, 100 pp. (in Hungarian).

Kuno, H. (1969). Pigeonite-bearing andesite and associated dacite from Asio, Japan. *American Journal of Science* **267**, 257–268.

Lantai, Cs. (1991). Genetics of garnets from andesites of the Karancs Mountains. *Acta Geologica Hungarica* **34**, 133–154.

Leake, B. E., Woolley, A. R., Arps, C. E. S., Birch, W. D., Gilbert, M. C., Grice, J. D., Hawthorne, F. C., Kato, A., Kisch, H. J., Krivovichev, V. G., Linthout, K., Laird, J., Mandarino, J. A., Maresch, W. V., Nickel, E. H., Rock, N. M. S., Schumacher, J. C., Smith, D. C., Stephenson, N. C. N., Ungaretti, L., Whittaker, J. W. & Youzhi, G. (1997). Nomenclature of amphiboles: report of the Subcommittee on Amphiboles of the International Mineralogical Association, Commission on New Minerals and Mineral Names. *American Mineralogist* **82**, 1019–1037.

Lexa, J. (1999). Outline of the Alpine geology and metallogeny of the Carpatho-Pannonian Region. In: Molnár, F., Lexa, J. & Hedenquist, J. W. (eds) *Epithermal Mineralization of the Western Carpathians. Society of Economic Geologists Guidebook Series* **31**, 65–108.

Lexa, J. & Konečný, V. (1974). The Carpathian Volcanic Arc: a discussion. *Acta Geologica Hungarica* **18**, 279–294.

Lexa, J., Konečný, V., Konečný, M. & Hojstricova, V. (1993). Distribúcia vulkanitov karpatsko-panónskeho regiónu v priestore a case. In: Rakús, M. & Vozár, J. (eds) *Geodynamicky model a hlbinná stavba Západnych Karpát. Geologicky ústav Dionyza Stura, Bratislava* 57–69 (in Slovak with English abstract).

López-Ruiz, J., Badiola, E. R. & Garcia Cacho, L. (1977). Origine des grenats des roches calco-alcalines du Sud-Est de l'Espagne. *Bulletin Volcanologique* **40**, 141–152.

Luth, R. W., Virgo, D., Boyd, F. R. & Wood, B. J. (1990). Ferric iron in mantle-derived garnets. *Contributions to Mineralogy and Petrology* **104**, 56–72.

Lyons, J. B. & Morse, S. A. (1970). Mg/Fe partitioning in garnet and biotite from some granitic, pelitic, and calcic rocks. *American Mineralogist* **55**, 231–245.

Maccarone, E. (1963). Aspetti geochimico-petrografico di alcuni exemplari di andesite granato-coriderittifera dell'Isola di Lipari. *Periodica Mineralogia* **32**, 277–302.

Mason, P. R. D. (1995). Petrogenesis of subduction-related volcanic rocks from the east Carpathians, Romania. Ph.D. thesis, University of London, 264 pp.

Mason, P. R. D., Downes, H., Thirlwall, M., Seghedi, I., Szakács, A., Lowry, D. & Mattey, D. (1996). Crustal assimilation as a major petrogenetic process in east Carpathian Neogene to Quaternary continental margin arc magmas. *Journal of Petrology* **37**, 927–959.

Mason, P. R. D., Seghedi, I., Szakács, A. & Downes, H. (1998). Magmatic constraints on geodynamic models of subduction in the Eastern Carpathians, Romania. *Tectonophysics* **297**, 157–176.

Mason, P. R. D., Kaspers, K. & van Bergen, M. J. (1999). Determination of sulfur isotope ratios and concentrations in water samples using ICP-MS incorporating hexapole ion optics. *Journal of Analytical Atomic Spectrometry* **14**, 1067–1074.

Mattey, D. & Macpherson, C. (1993). High-precision oxygen isotope microanalysis of ferromagnesian minerals by laser fluorination. *Chemical Geology* **105**, 305–318.

Maury, R. C., Clocchiatti, R., Coulon, C., D'Arco, P. & Westercamp, D. (1985). Signification du grenat et de la cordiérite dans les lavas du Sud-Ouest martiniquais. *Bulletin Minéralogique* **108**, 63–79.

Meulenkamp, J. E., Kovač, M. & Cicha, I. (1996). On Late Oligocene to Pliocene depocentre migration and the evolution of the Carpathian–Pannonian system. *Tectonophysics* **266**, 301–317.

Muhling, J. R. & Griffin, B. J. (1991). On recasting garnet analyses into end-member molecules—revisited. *Computers and Geosciences* **17**, 161–170.

Munksgaard, N. C. (1984). High $\delta^{18}O$ and possible pre-eruptional Rb–Sr isochrons in cordierite-bearing Neogene volcanics from SE Spain. *Contributions to Mineralogy and Petrology* **87**, 351–358.

Munksgaard, N. C. (1985). A non-magmatic origin for compositionally zoned euhedral garnets in silicic Neogene volcanics from SE Spain. *Neues Jahrbuch für Mineralogie, Monatshefte* **2**, 73–82.

Nakamura, N. (1974). Determination of REE, Ba, Mg, Na and K in carbonaceous and ordinary chondrites. *Geochimica et Cosmochimica Acta* **38**, 757–775.

Nemčok, M. & Lexa, J. (1990). Evolution of the Basin and Range structure around the Ziar Mountain Range. *Geologica Carpathica* **41**, 229–258.

Oliver, R. L. (1956). The origin of garnets in the Borrowdale Volcanic Series and associated rocks, English Lake District. *Geological Magazine* **93**, 121–139.

Pearce, J. A. & Parkinson, I. J. (1993). Trace element models for mantle melting: application to volcanic arc petrogenesis. In: Prichard, H. M., Alabaster, T., Harris, N. B. W. & Neary, C. R. (eds) *Magmatic Processes and Plate Tectonics. Geological Society, London, Special Publications* **76**, 373–403.

Pearce, N. J. G., Perkins, W. T., Westgate, J. A., Gorton, M. P., Jackson, S. E., Neal, C. R. & Chenery, S. P. (1997). A compilation of new and published major and trace element data for NIST SRM 610 and NIST SRM 612 glass reference materials. *Geostandards Newsletter* **21**, 115–144.

Pécskay, Z., Lexa, J., Szakács, A., Balogh, K., Seghedi, I., Konečný, V., Kovács, M., Márton, E., Kaliciak, M., Széky-Fux, V., Póka, T., Gyarmati, P., Edelstein, O., Rosu, E. & Zec, B. (1995). Space and time distribution of Neogene–Quaternary volcanism in the Carpatho-Pannonian Region. In: Downes, H. & Vaselli, O. (eds) *Neogene and Related Magmatism in the Carpatho-Pannonian Region. Special issue, Acta Vulcanologica* **7**, 15–28.

Popov, V. S., Boronikhin, V. A., Gmyra, V. G. & Semina, V. A. (1982). Garnets from the andesite–dacites of the Kel'sk volcanic highlands (Greater Caucasus). *International Geology Review* **24**, 577–584.

Smith, I. E. M., Ruddock, R. S. & Day, R. A. (1989). Miocene arc-type volcanic/plutonic complexes of the Northland Peninsula, New Zealand. *Royal Society of New Zealand Bulletin* **26**, 205–213.

Szabó, C. & Taylor, L. A. (1994). Mantle petrology and geochemistry beneath the Nógrád–Gömör Volcanic Field, Carpathian–Pannonian Region. *International Geology Review* **36**, 328–358.

Szabó, C., Harangi, S. & Csontos, L. (1992). Review of Neogene and Quaternary volcanism of the Carpathian–Pannonian region. In: Ziegler, P. A. (ed.) *Geodynamics of Rifting, Vol. I. Case Studies on Rifts: Europe and Asia. Tectonophysics* **208**, 243–256.

Szabó, C., Bodnar, R. J. & Sobolev, A. V. (1996). Metasomatism associated with subduction-related, volatile-rich silicate melt in the upper mantle beneath the Nógrád–Gömör Volcanic Field, Northern Hungary/Southern Slovakia: evidence from silicate melt inclusions. *European Journal of Mineralogy* **8**, 881–899.

Szabó, Zs., Harangi, S. & Weiszburg, T. (1999). Rock-forming garnet from the Csódi hill, Dunabogdány, Northern Hungary. *Topographia Mineralogica Hungariae, Miskolc* **6**, 87–102 (in Hungarian with English abstract).

Tari, G. & Horváth, F. (1995). Middle Miocene extensional collapse in the Alpine–Pannonian transition zone. In: Horváth, F., Tari, G. & Bokor, Cs. (eds) *Extensional Collapse of the Alpine Orogen and Hydrocarbon Prospects in the Basement and Basin Fill of the Western Pannonian Basin. AAPG International Conference and Exhibition, Nice, France, Guidebook to Fieldtrip No. 6, Hungary*, 75–105.

Taylor, H. P. & Coleman, R. G. (1968). $^{18}O/^{16}O$ ratios of coexisting minerals in glaucophane-bearing rocks. *Geological Society of America Bulletin* **79**, 1727–1756.

Thirlwall, M. F. (1991). Long-term reproducibility of multicollector Sr and Nd isotope ratio analysis. *Chemical Geology* **94**, 85–104.

Thirlwall, M. F. & Fitton, J. G. (1983). Sm–Nd garnet age for the Ordovician Borrowdale Volcanic Group, English Lake District. *Journal of the Geological Society, London* **140**, 511–518.

Tsvetkov, A. A. & Borisovskiy, S. Y. (1980). High-pressure minerals in Jurassic andesite–dacite lavas from Northern Osetia. *International Geology Review* **22**, 297–306.

Ujike, O. & Onuki, H. (1976). Phenocrystic hornblendes from Tertiary andesites and dacites. Kagawa Prefecture. *Journal of the Japan Association: Mineralogy, Petrology and Economic Geology* **71**, 389–399.

Walsh, J. N., Buckley, F. & Barker, J. (1981). The simultaneous determination of the REE in rocks using inductively coupled plasma source spectrometer. *Chemical Geology* **33**, 141–153.

Westercamp, D. (1976). Pétrologie de la dacite à grenat de Gros Ilet, Martinique, Petites Antilles françaises. *Bulletin du BRGM, 2e série, Section IV* **4**, 253–265.

Wood, C. P. (1974). Petrogenesis of garnet-bearing rhyolites from Canterbury, New Zealand. *New Zealand Journal of Geology and Geophysics* **17**, 759–787.

Zeck, H. P. (1970). An erupted migmatite from Cerro del Hoyazo, SE Spain. *Contributions to Mineralogy and Petrology* **26**, 225–246.

Zeck, H. P. (1992). Restite–melt and mafic–felsic magma mixing and mingling in an S-type dacite, Cerro del Hoyazo, southeastern Spain. *Transactions of the Royal Society of Edinburgh: Earth Sciences* **83**, 139–144.

Zeck, H. P. (1999). Alpine kinematics in the western Mediterranean: a westward-directed subduction regime followed by slab roll-back and slab detachment. In: Durand, B., Jolivet, L., Horváth, F. & Séranne, M. (eds) *The Mediterranean Basins: Tertiary Extension within the Alpine Orogen. Geological Society, London, Special Publications* **156**, 109–120.